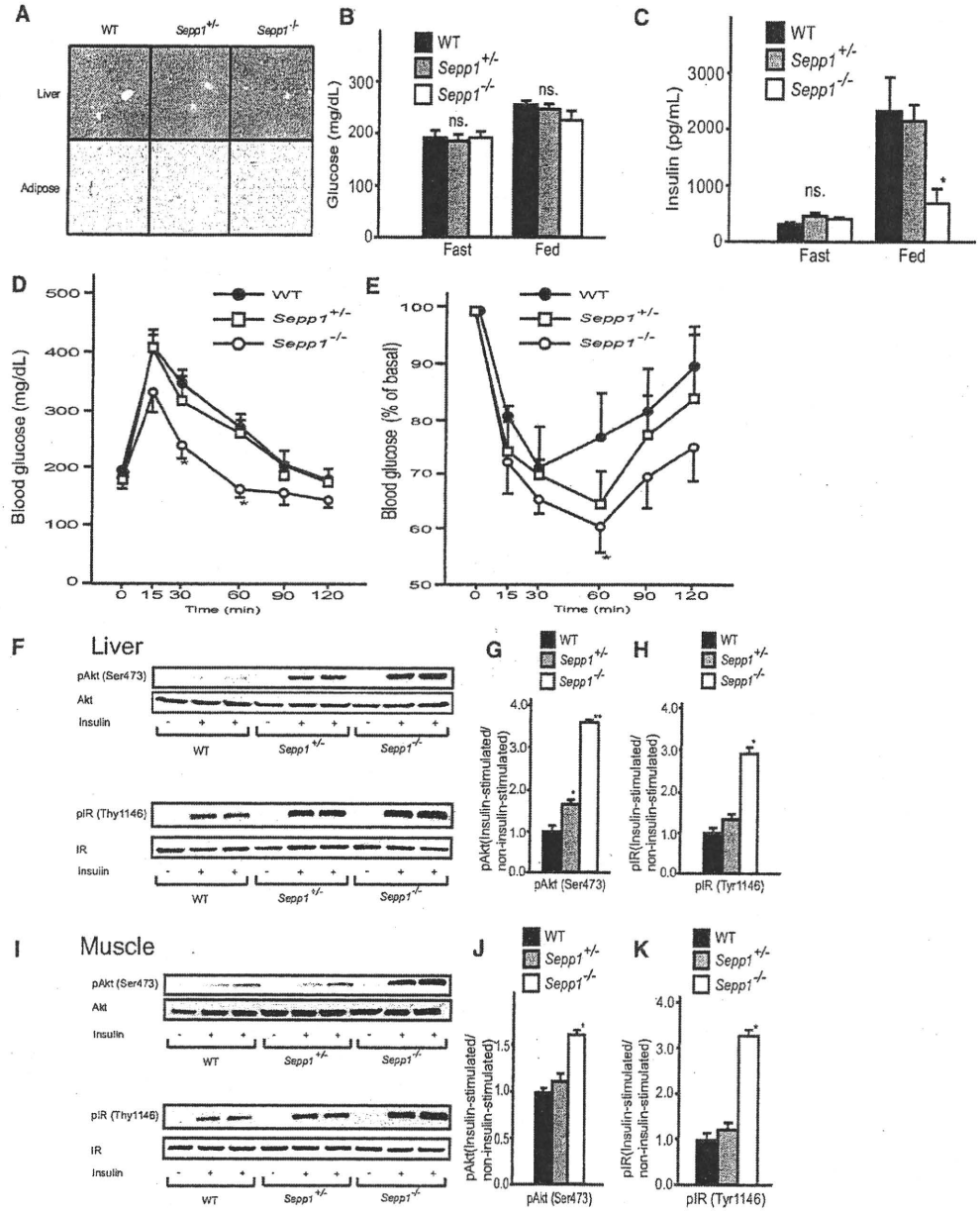

Figure 5. *Sepp1*-Deficient Mice Show Improved Glucose Tolerance and Enhanced Insulin Sensitivity

(A) Hematoxylin-and-eosin-stained liver and epididymal fat sections from male *Sepp1*$^{+/-}$ and *Sepp1*$^{-/-}$ mice.

(B) Blood glucose levels in *Sepp1*-deficient mice (n = 7). The mice were fasted for 6 hr.

(C) Blood insulin levels in *Sepp1*-deficient mice (n = 7).

(D and E) Intraperitoneal glucose (D) and insulin (E) tolerance tests in male *Sepp1*-deficient mice (n = 7). Glucose and insulin were administered at doses of 1.5 g/kg body weight and 4 units/kg body weight, respectively.

(F–K) Western blot analysis of phosphorylated Akt (pAkt) and phosphorylated insulin receptor (pIR) in liver (F–H) and skeletal muscle (I–K). Mice (n = 6) were stimulated with insulin (administered intraperitoneally). At 20 min after insulin stimulation, mice were anesthetized, and liver and hind-limb muscle samples removed for analysis.

Data in (B)–(E), (G), (H), (J), and (K) represent the means ± SEM from six to seven mice per group. *$p < 0.05$, **$p < 0.01$ versus wild-type mice. See also Figure S3.

siRNA Injection into KKAy mice

Delivery of siRNA targeted to the liver was performed by tail vein injections into mice, via hydrodynamic techniques, as previously described (McCaffrey et al., 2002; Zender et al., 2003). For these experiments, KKAy mice at 7–8 weeks of age (31–33 g body weight) were used. Mice were anesthetized with pentobarbital, and 2 nmol of siRNA, diluted in 3 ml of PBS, was injected into the tail vein over 15–20 s. All siRNAs were purchased from Applied Biosystems (Silencer^{R} In Vivo Ready Pre-designed siRNA). *Sepp1* siRNAs with the following

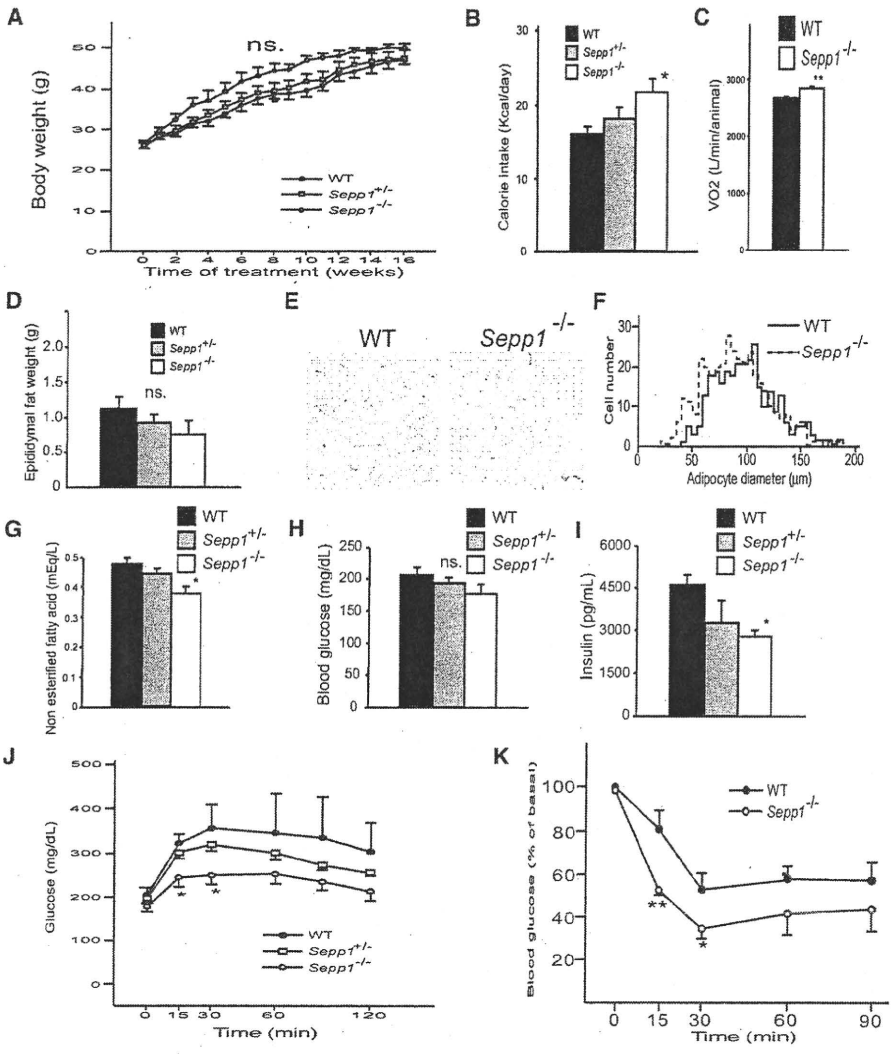

Figure 6. *Sepp1*-Deficient Mice Are Protected from Diet-Induced Insulin Resistance and Adipocyte Hypertrophy

(A) Body weight of *Sepp1*-deficient and wild-type mice fed a high-fat, high-sucrose diet (HFHSD; n = 4–8). Sixteen-week-old male mice were fed a HFHSD for 16 weeks.

(B) Daily calorie intake in *Sepp1*-deficient and wild-type mice (n = 4–8).

(C) Energy expenditure (as measured by VO_2 consumption through indirect calorimetry; n = 4).

(D) Epididymal fat mass in *Sepp1*-deficient and wild-type mice fed HFHSD (n = 4–7).

(E) Hematoxylin-and-eosin-stained epididymal fat sections from wild-type and *Sepp1*$^{-/-}$ mice.

(F) Histogram showing adipocyte diameters. We determined adipocyte diameters by measuring at least 300 adipocytes randomly selected from four independent sections.

(G) Blood nonestimated fatty acid levels in *Sepp1*-deficient and wild-type mice fed HFHSD (n = 4–7).

(H) Blood glucose levels in *Sepp1*-deficient and wild-type mice fed HFHSD (n = 4–8).

(I) Blood insulin levels in *Sepp1*-deficient and wild-type mice fed HFHSD (n = 4–8). Blood samples were obtained from mice fed a HFHSD for 16 weeks after a 12 hr fast in (G)–(I).

(J) Intraperitoneal glucose tolerance tests in wild-type and *Sepp1*-deficient mice (n = 4–8). Glucose was administered at a dose of 0.3 g/kg body weight.

(K) Intraperitoneal insulin tolerance tests in wild-type and *Sepp1*-deficient mice (n = 5–10). Insulin was administered at a dose of 2.0 units/kg body weight.

Data in (A)–(D) and (G)–(K) represent the means ± SEM from four to ten mice per group. *$p < 0.05$, **$p < 0.01$ versus wild-type mice. See also Figure S4.

sequence were synthesized: mouse *Sepp1*, 5′-GGUGUCAGAACACAUC GCAtt-3′ (sense). Negative control siRNA was also used and had no significant homology with any known gene sequences in mouse, rat, or human. Glucose and insulin loading tests were performed 2–7 days after injection of mice with siRNA.

SeP Knockout Mice

SeP knockout mice were produced by homologous recombination with genomic DNA cloned from an Sv-129 P1 library, as described previously (Hill et al., 2003). As female SeP knockout mice had inconsistent phenotypes, only male mice were used in this study.

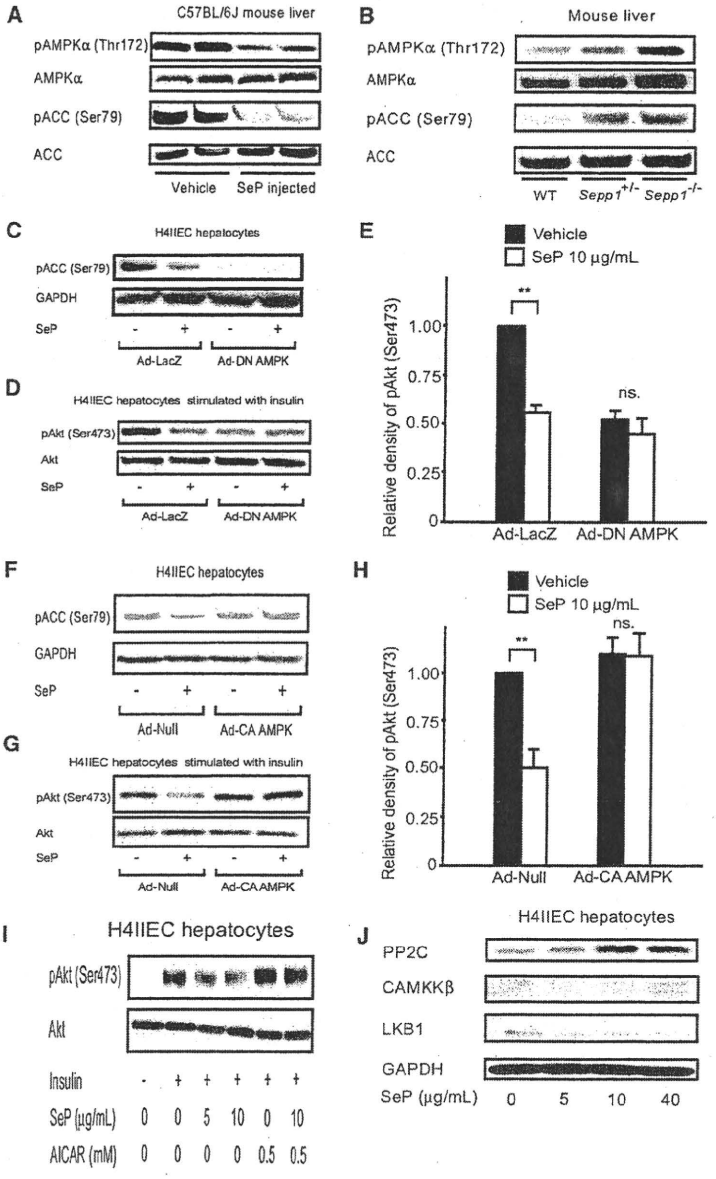

Figure 7. SeP Reduces Phosphorylation of AMPK and ACC in Hepatocytes

(A) Phosphorylation of AMPK and ACC in the liver of mice injected with SeP or vehicle. C57BL/6J mice were injected intravenously with purified human SeP (1 mg/kg body weight) or vehicle (phosphate-buffered saline). At 6 hr after injection, the liver was removed.

(B) Phosphorylation of AMPK and ACC in the liver of *Sepp1*-deficient mice after a 12 hr fast.

(C–E) Effects of dominant-negative AMPK on ACC phosphorylation (C) and insulin-stimulated Akt phosphorylation (D and E) in H4IIEC hepatocytes treated with SeP.

(F–H) Effects of constitutively active AMPK on ACC phosphorylation (F) and insulin-stimulated Akt phosphorylation (G and H) in H4IIEC hepatocytes treated with SeP.

(I) Effect of AICAR on SeP-induced insulin resistance in H4IIEC hepatocytes.

(J) Levels of PP2C, CaMKKβ, and LKB1 in H4IIEC hepatocytes treated with various concentrations of SeP for 12 hr.

Data in (E) and (H) represent the means ± SEM from three independent experiments. **$p < 0.01$ versus vehicle-treated cells. See also Figure S5.

Statistical Analyses

All data were analyzed using the Japanese Windows Edition of the Statistical Package for Social Science (SPSS) Version 11.0. Numeric values are reported as the mean ± SEM. Differences between two groups were assessed with unpaired two-tailed t tests. Data involving more than two groups were assessed by analysis of variance (ANOVA). Glucose and insulin tolerance tests were examined with repeated-measures ANOVA.

ACCESSION NUMBERS

Microarray data have been deposited in Gene Expression Omnibus under accession number GSE23343.

SUPPLEMENTAL INFORMATION

Supplemental Information includes Supplemental Experimental Procedures, five figures, and five tables and can be found with this article online at doi:10.1016/j.cmet.2010.09.015.

ACKNOWLEDGMENTS

We thank Kuniaki Arai of Kanazawa University for liver biopsies and Isao Usui, Hajime Ishihara, and Toshiyasu Sasaoka of Toyama University for supplying their technical expertise on Western blot analyses of phosphoproteins. We thank Yuriko Furuta and Yoko Hashimoto for technical assistance. We thank Fabienne Foufelle of Université Pierre et Marie Curie for providing adenovirus vector encoding DN-AMPK. We are indebted to Kristina E. Hill and Raymond F. Burk of Vanderbilt University School of Medicine for the *Sepp1* knockout mice. This work was supported by Takeda Science Foundation and Grants-in-Aid from the Ministry of Education, Culture, Sports, Science and Technology, Japan. We also thank Cathie Chung for editing the manuscript.

Received: February 2, 2009
Revised: April 29, 2010
Accepted: August 13, 2010
Published: November 2, 2010

REFERENCES

Andoh, A., Hirashima, M., Maeda, H., Hata, K., Inatomi, O., Tsujikawa, T., Sasaki, M., Takahashi, K., and Fujiyama, Y. (2005). Serum selenoprotein-P levels in patients with inflammatory bowel disease. Nutrition *21*, 574–579.

Auberger, P., Falquerho, L., Contreres, J.O., Pages, G., Le Cam, G., Rossi, B., and Le Cam, A. (1989). Characterization of a natural inhibitor of the insulin receptor tyrosine kinase: cDNA cloning, purification, and anti-mitogenic activity. Cell *58*, 631–640.

Bellinger, F.P., He, Q.P., Bellinger, M.T., Lin, Y., Raman, A.V., White, L.R., and Berry, M.J. (2008). Association of selenoprotein p with Alzheimer's pathology in human cortex. J. Alzheimers Dis. *15*, 465–472.

Bleys, J., Navas-Acien, A., and Guallar, E. (2007). Serum selenium and diabetes in U.S. adults. Diabetes Care *30*, 829–834.

Burk, R.F., and Hill, K.E. (2005). Selenoprotein P: an extracellular protein with unique physical characteristics and a role in selenium homeostasis. Annu. Rev. Nutr. *25*, 215–235.

Burk, R.F., Hill, K.E., Olson, G.E., Weeber, E.J., Motley, A.K., Winfrey, V.P., and Austin, L.M. (2007). Deletion of apolipoprotein E receptor-2 in mice lowers brain selenium and causes severe neurological dysfunction and death when a low-selenium diet is fed. J. Neurosci. *27*, 6207–6211.

Carlson, B.A., Novoselov, S.V., Kumaraswamy, E., Lee, B.J., Anver, M.R., Gladyshev, V.N., and Hatfield, D.L. (2004). Specific excision of the selenocysteine tRNA[Ser]Sec (Trsp) gene in mouse liver demonstrates an essential role of selenoproteins in liver function. J. Biol. Chem. *279*, 8011–8017.

Davies, S.P., Helps, N.R., Cohen, P.T., and Hardie, D.G. (1995). 5′-AMP inhibits dephosphorylation, as well as promoting phosphorylation, of the AMP-activated protein kinase. Studies using bacterially expressed human protein phosphatase-2C alpha and native bovine protein phosphatase-2AC. FEBS Lett. *377*, 421–425.

Després, J.P., Lamarche, B., Mauriège, P., Cantin, B., Dagenais, G.R., Moorjani, S., and Lupien, P.J. (1996). Hyperinsulinemia as an independent risk factor for ischemic heart disease. N. Engl. J. Med. *334*, 952–957.

Friedman, J.M., and Halaas, J.L. (1998). Leptin and the regulation of body weight in mammals. Nature *395*, 763–770.

Hill, K.E., Zhou, J., McMahan, W.J., Motley, A.K., Atkins, J.F., Gesteland, R.F., and Burk, R.F. (2003). Deletion of selenoprotein P alters distribution of selenium in the mouse. J. Biol. Chem. *278*, 13640–13646.

Kahn, B.B., Alquier, T., Carling, D., and Hardie, D.G. (2005). AMP-activated protein kinase: ancient energy gauge provides clues to modern understanding of metabolism. Cell Metab. *1*, 15–25.

Kawano, K., Hirashima, T., Mori, S., Saitoh, Y., Kurosumi, M., and Natori, T. (1992). Spontaneous long-term hyperglycemic rat with diabetic complications. Otsuka Long-Evans Tokushima Fatty (OLETF) strain. Diabetes *41*, 1422–1428.

Maeda, K., Okubo, K., Shimomura, I., Funahashi, T., Matsuzawa, Y., and Matsubara, K. (1996). cDNA cloning and expression of a novel adipose specific collagen-like factor, apM1 (AdiPose Most abundant Gene transcript 1). Biochem. Biophys. Res. Commun. *221*, 286–289.

Maeda, N., Shimomura, I., Kishida, K., Nishizawa, H., Matsuda, M., Nagaretani, H., Furuyama, N., Kondo, H., Takahashi, M., Arita, Y., et al. (2002). Diet-induced insulin resistance in mice lacking adiponectin/ACRP30. Nat. Med. *8*, 731–737.

Masiulis, I., Quill, T.A., Burk, R.F., and Herz, J. (2009). Differential functions of the Apoer2 intracellular domain in selenium uptake and cell signaling. Biol. Chem. *390*, 67–73.

McCaffrey, A.P., Meuse, L., Pham, T.T., Conklin, D.S., Hannon, G.J., and Kay, M.A. (2002). RNA interference in adult mice. Nature *418*, 38–39.

Minokoshi, Y., Kim, Y.B., Peroni, O.D., Fryer, L.G., Müller, C., Carling, D., and Kahn, B.B. (2002). Leptin stimulates fatty-acid oxidation by activating AMP-activated protein kinase. Nature *415*, 339–343.

Misu, H., Takamura, T., Matsuzawa, N., Shimizu, A., Ota, T., Sakurai, M., Ando, H., Arai, K., Yamashita, T., Honda, M., et al. (2007). Genes involved in oxidative phosphorylation are coordinately upregulated with fasting hyperglycaemia in livers of patients with type 2 diabetes. Diabetologia *50*, 268–277.

Oike, Y., Akao, M., Yasunaga, K., Yamauchi, T., Morisada, T., Ito, Y., Urano, T., Kimura, Y., Kubota, Y., Maekawa, H., et al. (2005). Angiopoietin-related growth factor antagonizes obesity and insulin resistance. Nat. Med. *11*, 400–408.

Olson, G.E., Winfrey, V.P., Nagdas, S.K., Hill, K.E., and Burk, R.F. (2007). Apolipoprotein E receptor-2 (ApoER2) mediates selenium uptake from selenoprotein P by the mouse testis. J. Biol. Chem. *282*, 12290–12297.

Ota, T., Takamura, T., Kurita, S., Matsuzawa, N., Kita, Y., Uno, M., Akahori, H., Misu, H., Sakurai, M., Zen, Y., et al. (2007). Insulin resistance accelerates a dietary rat model of nonalcoholic steatohepatitis. Gastroenterology *132*, 282–293.

Persson-Moschos, M., Alfthan, G., and Akesson, B. (1998). Plasma selenoprotein P levels of healthy males in different selenium status after oral supplementation with different forms of selenium. Eur. J. Clin. Nutr. *52*, 363–367.

Saito, Y., and Takahashi, K. (2002). Characterization of selenoprotein P as a selenium supply protein. Eur. J. Biochem. *269*, 5746–5751.

Saito, Y., Hayashi, T., Tanaka, A., Watanabe, Y., Suzuki, M., Saito, E., and Takahashi, K. (1999). Selenoprotein P in human plasma as an extracellular phospholipid hydroperoxide glutathione peroxidase. Isolation and enzymatic characterization of human selenoprotein p. J. Biol. Chem. *274*, 2866–2871.

Saito, Y., Watanabe, Y., Saito, E., Honjoh, T., and Takahashi, K. (2001). Production and application of monoclonal antibodies to human selenoprotein P. J. Health Sci. *47*, 346–352.

Saltiel, A.R., and Kahn, C.R. (2001). Insulin signalling and the regulation of glucose and lipid metabolism. Nature *414*, 799–806.

Scherer, P.E., Williams, S., Fogliano, M., Baldini, G., and Lodish, H.F. (1995). A novel serum protein similar to C1q, produced exclusively in adipocytes. J. Biol. Chem. *270*, 26746–26749.

Schomburg, L., Schweizer, U., Holtmann, B., Flohé, L., Sendtner, M., and Köhrle, J. (2003). Gene disruption discloses role of selenoprotein P in selenium delivery to target tissues. Biochem. J. *370*, 397–402.

Speckmann, B., Walter, P.L., Alili, L., Reinehr, R., Sies, H., Klotz, L.O., and Steinbrenner, H. (2008). Selenoprotein P expression is controlled through interaction of the coactivator PGC-1alpha with FoxO1a and hepatocyte nuclear factor 4alpha transcription factors. Hepatology *48*, 1998–2006.

Srinivas, P.R., Wagner, A.S., Reddy, L.V., Deutsch, D.D., Leon, M.A., Goustin, A.S., and Grunberger, G. (1993). Serum alpha 2-HS-glycoprotein is an inhibitor of the human insulin receptor at the tyrosine kinase level. Mol. Endocrinol. *7*, 1445–1455.

Steinberg, G.R., Michell, B.J., van Denderen, B.J., Watt, M.J., Carey, A.L., Fam, B.C., Andrikopoulos, S., Proietto, J., Görgün, C.Z., Carling, D., et al. (2006). Tumor necrosis factor alpha-induced skeletal muscle insulin resistance involves suppression of AMP-kinase signaling. Cell Metab. *4*, 465–474.

Steppan, C.M., Bailey, S.T., Bhat, S., Brown, E.J., Banerjee, R.R., Wright, C.M., Patel, H.R., Ahima, R.S., and Lazar, M.A. (2001). The hormone resistin links obesity to diabetes. Nature *409*, 307–312.

Takamura, T., Sakurai, M., Ota, T., Ando, H., Honda, M., and Kaneko, S. (2004). Genes for systemic vascular complications are differentially expressed in the livers of type 2 diabetic patients. Diabetologia *47*, 638–647.

Takeda, S., Sato, N., Uchio-Yamada, K., Sawada, K., Kunieda, T., Takeuchi, D., Kurinami, H., Shinohara, M., Rakugi, H., and Morishita, R. (2010). Diabetes-accelerated memory dysfunction via cerebrovascular inflammation and Abeta deposition in an Alzheimer mouse model with diabetes. Proc. Natl. Acad. Sci. USA *107*, 7036–7041.

Takeshita, Y., Takamura, T., Hamaguchi, E., Shimizu, A., Ota, T., Sakurai, M., and Kaneko, S. (2006). Tumor necrosis factor-alpha-induced production of plasminogen activator inhibitor 1 and its regulation by pioglitazone and cerivastatin in a nonmalignant human hepatocyte cell line. Metabolism *55*, 1464–1472.

Velculescu, V.E., Zhang, L., Vogelstein, B., and Kinzler, K.W. (1995). Serial analysis of gene expression. Science *270*, 484–487.

Walter, P.L., Steinbrenner, H., Barthel, A., and Klotz, L.O. (2008). Stimulation of selenoprotein P promoter activity in hepatoma cells by FoxO1a transcription factor. Biochem. Biophys. Res. Commun. *365*, 316–321.

Xu, A., Lam, M.C., Chan, K.W., Wang, Y., Zhang, J., Hoo, R.L., Xu, J.Y., Chen, B., Chow, W.S., Tso, A.W., and Lam, K.S. (2005). Angiopoietin-like protein 4 decreases blood glucose and improves glucose tolerance but induces hyperlipidemia and hepatic steatosis in mice. Proc. Natl. Acad. Sci. USA *102*, 6086–6091.

Yamauchi, T., Kamon, J., Minokoshi, Y., Ito, Y., Waki, H., Uchida, S., Yamashita, S., Noda, M., Kita, S., Ueki, K., et al. (2002). Adiponectin stimulates glucose utilization and fatty-acid oxidation by activating AMP-activated protein kinase. Nat. Med. *8*, 1288–1295.

Yang, Q., Graham, T.E., Mody, N., Preitner, F., Peroni, O.D., Zabolotny, J.M., Kotani, K., Quadro, L., and Kahn, B.B. (2005). Serum retinol binding protein 4 contributes to insulin resistance in obesity and type 2 diabetes. Nature *436*, 356–362.

Zender, L., Hutker, S., Liedtke, C., Tillmann, H.L., Zender, S., Mundt, B., Waltemathe, M., Gosling, T., Flemming, P., Malek, N.P., et al. (2003). Caspase 8 small interfering RNA prevents acute liver failure in mice. Proc. Natl. Acad. Sci. USA *100*, 7797–7802.

Research Article

EASL EUROPEAN ASSOCIATION FOR THE STUDY OF THE LIVER | JOURNAL OF HEPATOLOGY

Differential interferon signaling in liver lobule and portal area cells under treatment for chronic hepatitis C

Masao Honda[1,2], Mikiko Nakamura[1], Makoto Tateno[1], Akito Sakai[1], Tetsuro Shimakami[1], Takayoshi Shirasaki[1], Tatsuya Yamashita[1], Kuniaki Arai[1], Taro Yamashita[1], Yoshio Sakai[1], Shuichi Kaneko[1,*]

[1]*Department of Gastroenterology, Kanazawa University, Graduate School of Medicine, Kanazawa, Japan;* [2]*Department of Advanced Medical Technology, Kanazawa University, Graduate School of Health Medicine, Kanazawa, Japan*

Background & Aims: The mechanisms of treatment resistance to interferon (IFN) and ribavirin (Rib) combination therapy for hepatitis C virus (HCV) infection are not known. This study aims to gain insight into these mechanisms by exploring hepatic gene expression before and during treatment.

Methods: Liver biopsy was performed in 50 patients before therapy and repeated in 30 of them 1 week after initiating combination therapy. The cells in liver lobules (CLL) and the cells in portal areas (CPA) were obtained from 12 patients using laser capture microdissection (LCM).

Results: Forty-three patients were infected with genotype 1 HCV, 20 of who were viral responders (genotype 1-Rsp) with treatment outcome of SVR or TR, while 23 were non-responders (genotype 1-nonRsp) with NR. Only seven patients were infected with genotype 2. Before treatment, the expression of *IFN and Rib-stimulated genes* (IRSGs), apoptosis-associated genes, and immune reaction gene pathways was greater in genotype 1-nonRsp than in Rsp. During treatment, IRSGs were induced in genotype 1-Rsp, but not in nonRsp. IRSG induction was irrelevant in genotype 2-Rsp and was mainly impaired in CLL but not in CPA. Pathway analysis revealed that many immune regulatory pathways were induced in CLL from genotype 1-Rsp, while growth factors related to angiogenesis and fibrogenesis were more induced in CPA from genotype 1-nonRsp.

Conclusions: Impaired IRSGs induction in CLL reduces the sensitivity to treatment for genotype 1 HCV infection. CLL and CPA in the liver might be differentially involved in treatment resistance. These findings could be useful for the improvement of therapy for HCV infection.

Introduction

A human liver infected with hepatitis C virus (HCV) develops chronic hepatitis, cirrhosis, and in some instances, hepatocellular carcinoma (HCC). Although interferon (IFN) and ribavirin (Rib) combination therapy has become a popular modality for treating patients with chronic hepatitis C (CH-C), about 50% of patients relapse, particularly those with genotype 1b and high viral load [8]. The reasons for treatment failure are poorly understood. Many studies of IFN and Rib combination therapy for CH-C suggested that patients who cleared HCV viremia early during therapy tended to show favorable outcomes. On the other hand, patients who needed a longer period to clear HCV had poorer outcomes [4,7,17], and those who showed no response (no or minimal decrease in HCV-RNA) to IFN and Rib combination therapy hardly ever achieved a sustained viral response (SVR).

To elucidate the underlying mechanism of treatment resistance, expression profiles in the liver [3,6,20] and peripheral mononuclear cells (PBMC) [10,21] during IFN treatment for CH-C patients have been examined. In chronic viral hepatitis, increased numbers of immune regulatory cells infiltrate the liver. These liver-infiltrating lymphocytes (LILs) might play important roles for virus eradication and are potentially linked to treatment outcome. Previously, we selectively isolated cells in liver lobules (CLL) and cells in the portal area (CPA) from biopsy specimens using laser capture microdissection (LCM) and analyzed their gene expression profiles [11,19]. From these profile analyses, it could be inferred that the majority of CLL were hepatocytes and the majority of CPA were lymphocytes, although other cellular components such as Kupffer cells, endothelial cells, myofibroblasts, and bile duct cells co-existed as well.

To gain further insight into the mechanisms of therapy resistance, we analyzed expression profiles in CLL and CPA in addition to whole liver tissues during IFN therapy for CH-C.

Keywords: HCV; IFN; LCM; Gene expression.
Received 12 October 2009; received in revised form 29 April 2010; accepted 30 April 2010; available online 15 July 2010

* Corresponding author. Address: Department of Gastroenterology, Kanazawa University, Graduate School of Medicine, Takara-Machi 13-1, Kanazawa 920-8641, Japan. Tel.: +81 76 265 2235; fax: +81 76 234 4250.
E-mail address: skaneko@m-kanazawa.jp (S. Kaneko).

Abbreviations: HCV, hepatitis C virus; HBV, hepatitis B virus; miRNA, micro RNA; CH-B, chronic hepatitis B; CH-C, chronic hepatitis C; HCC-B, hepatitis B-related hepatocellular carcinoma; HCC-C, hepatitis C-related hepatocellular carcinoma; OCT, optimum cutting temperature.

Research Article

Materials and methods

Patients

Patients with CH-C were enrolled in this study at the Graduate School of Medicine, Kanazawa University Hospital, Japan, between 2001 and 2007 (Tables 1 and 2). Prior to the study, we obtained the required approvals, namely: informed consent from all participating patients and ethics approval from the ethics committee for human genome/gene analysis research at Kanazawa University Graduate School of Medical Science. Thirty patients were administered IFN-α 2b (6 MU; every day for 2 weeks, then three times a week for 22 weeks) (Schering-Plough K.K., Tokyo, Japan) and Rib (10–13 mg/kg/day) combination therapy for 24 weeks (Table 1). Twenty patients were administered Peg-IFN-α 2b and Rib combination therapy for 48 weeks (Table 2). The final outcome of the treatment was assessed at 24 weeks after cessation of the combination therapy. In addition, 10 samples of normal liver tissues obtained during surgery for metastatic liver cancer were used as controls.

We defined treatment outcomes according to the decrease in viremia as follows: sustained viral response (SVR), clearance of HCV viremia at 24 weeks after cessation of therapy; transient response (TR), no detectable HCV viremia at 24 weeks but relapse during the follow-up period; and nonresponse (NR), HCV viremia detected at the cessation of therapy. We defined a patient who achieved SVR or TR as a viral responder (Rsp) and a patient who exhibited an NR as a non-responder (nonRsp). As patient 10 stopped treatment at 5 weeks due to an adverse side effect, we grouped this patient as Rsp based on the observed viral decline within 2 weeks (Table 1).

HCV genotype was classified by the methods described by Okamoto et al. [16] Twenty-three patients were infected with genotype 1b and seven patients were infected with genotype 2 (2a; 6, 2b; 1) (Tables 1 and 2).

Patient serum was aliquoted and stored at −20 °C until use. HCV-RNA was serially monitored by quantitative real-time detection (RTD)-PCR (COBAS® AmpliPrep/COBAS® TaqMan® System®) [9] before treatment, at 48 h, 2 weeks and 24 weeks after initiation of therapy and at 24 weeks after cessation of therapy.

The grading and staging of chronic hepatitis were histologically assessed according to the method described by Desmet et al. (Table 1) [5].

Table 1. Characteristics of study patients who received IFN and ribavirin combination therapy.

				ALT (IU/ml)		Liver histology			HCV-RNA (Log IU/ml)				Viral kinetics			
Pt.No.	Sex	Age (yr)	Genotype	Before therapy	During therapy	Before therapy F A	During therapy F A	LCM	Before therapy	48 h	2 wk	24 wk	1st phase delinie Log/24 h	2nd phase decline Log/week	Viral response	Outcome
1	M	48	1b	83	45	1 1	1 1	+	6.6	4.5	3.5	-	1.1	0.5	Rsp	SVR
2	M	32	1b	192	95	1 1	1 1	-	6.4	3.9	3.2	-	1.3	0.4	Rsp	SVR
3	F	50	1b	57	37	1 1	1 1	-	5.8	2.5	1.5	-	1.7	0.5	Rsp	TR
4	M	36	1b	119	117	1 1	1 1	+	6.1	4.4	4.2	+	0.9	0.1	nonRsp	NR
5	M	54	1b	82	69	1 1	1 1	-	6.6	5.1	3.9	+	0.8	0.6	nonRsp	NR
6	M	43	1b	143	116	1 1	1 1	-	6.3	4.4	4.1	+	1.0	0.2	nonRsp	NR
7	M	48	1b	33	30	1 1	1 1	+	1.5	0.0	0.0	-	>0.8	-	Rsp	SVR
8	M	52	1b	316	374	1 2	1 1	-	4.7	5.1	3.9	+	-0.2	0.6	nonRsp	NR
9	M	45	1b	112	39	1 0	2 0	-	6.2	5.1	5.7	+	0.6	-0.3	nonRsp	NR
10	M	48	1b	48	30	2 2	2 1	+	6.4	4.0	2.6	NA	1.2	0.8	Rsp	NA
11	M	52	1b	114	80	2 2	2 1	-	6.1	3.7	3.0	-	1.2	0.4	Rsp	TR
12	F	63	1b	38	30	2 1	2 1	-	5.2	4.2	4.5	+	0.5	-0.2	nonRsp	NR
13	M	58	1b	90	83	2 2	2 2	+	6.9	4.9	5.6	+	1.0	-0.4	nonRsp	NR
14	F	61	1b	87	43	2 1	2 1	+	6.5	3.9	3.7	+	1.3	0.1	nonRsp	NR
15	F	64	1b	133	111	2 1	3 2	-	6.0	4.4	3.6	+	0.8	0.4	nonRsp	NR
16	F	62	1b	251	159	3 2	3 2	-	4.8	2.7	1.5	-	1.1	0.6	Rsp	SVR
17	M	54	1b	211	205	3 2	3 2	+	6.7	0.0	0.0	-	>3.4	-	Rsp	SVR
18	F	68	1b	153	145	3 2	3 2	+	4.9	4.3	3.5	+	0.3	0.4	nonRsp	NR
19	F	69	1b	64	43	3 2	3 2	-	4.4	1.5	0.0	-	1.5	0.8	Rsp	SVR
20	M	49	1b	91	83	3 2	3 2	+	6.6	4.2	3.8	+	1.2	0.2	nonRsp	NR
21	M	55	1b	187	196	4 1	4 2	-	5.8	5.1	5.6	+	0.4	-0.3	nonRsp	NR
22	F	45	1b	113	75	4 2	3 3	-	5.7	4.2	2.7	-	0.8	0.8	Rsp	TR
23	M	60	1b	86	49	4 2	3 1	-	6.3	3.5	3.5	+	1.4	0.0	nonRsp	NR
24	F	51	2b	98	90	1 1	1 1	-	2.7	1.5	0.0	-	0.6	0.8	Rsp	SVR
25	M	37	2a	241	211	1 0	1 0	-	4.0	1.5	0.0	-	1.3	0.8	Rsp	SVR
26	F	45	2a	91	33	2 1	2 1	-	5.4	2.2	1.5	-	1.6	0.4	Rsp	TR
27	M	46	2a	101	45	2 1	2 1	+	3.6	0.0	0.0	-	>1.8	-	Rsp	SVR
28	M	54	2a	196	177	3 2	2 1	+	4.2	0.0	0.0	-	>2.1	-	Rsp	SVR
29	F	68	2a	234	135	3 1	3 2	+	4.6	3.1	0.0	-	0.8	1.7	Rsp	SVR
30	M	67	2a	155	163	4 2	4 2	-	3.9	1.5	0.0	-	1.2	0.8	Rsp	SVR

First phase decline was determined by subtracting HCV-RNA at 48 h from before therapy.
Second phase decline was determined by subtracting HCV-RNA at 2 wk from 48 h.
NA, not applicable; LCM, laser capture microdissection; ALT, alanine aminotransferase; SVR, sustained viral response; A, activity; NR, nonresponse; F, fibrosis; TR, transient response; Rsp, viral responder, patients with SVR or TR; nonRsp, non-viral responder; patients with NR; HCV-RNA was assayed by COBAS® AmpliPrep/COBAS® TaqMan® System® (Log IU/mL).

Table 2. Characteristics of patients who received Peg-IFN and ribavirin combination therapy and normal control.

Pt.No.	Sex	Age (yr)	Genotype	ALT (IU/ml)	Liver histology		HCV-RNA (Log IU/ml)				Viral response	Outcome
				Before therapy	Before therapy		Before therapy	2 wk	4 wk	24 wk		
					F	A						
1	M	57	1b	68	1	1	6.5	-	-	-	Rsp	SVR
2	F	56	1b	31	1	1	6.5	4.4	-	-	Rsp	SVR
3	M	63	1b	50	1	1	6.1	-	-	-	Rsp	SVR
4	M	44	1b	45	1	1	6.5	3.7	-	-	Rsp	SVR
5	F	51	1b	27	2	1	6.5	4.1	-	-	Rsp	SVR
6	M	58	1b	72	2	1	6.2	-	-	-	Rsp	SVR
7	M	60	1b	71	2	2	6.2	3.9	-	-	Rsp	SVR
8	F	52	1b	58	2	2	6.5	4.1	-	-	Rsp	SVR
9	F	62	1b	60	3	2	5.9	3.8	-	-	Rsp	SVR
10	M	55	1b	106	3	2	6.4	-	-	-	Rsp	SVR
11	M	30	1b	31	1	1	6.4	6.1	5.9	+	nonRsp	NR
12	F	55	1b	23	1	2	6.5	6.1	5.9	+	nonRsp	NR
13	M	58	1b	129	1	2	6.3	6.0	5.8	+	nonRsp	NR
14	M	42	1b	326	2	1	6.6	6.2	5.8	+	nonRsp	NR
15	F	61	1b	77	2	1	6.1	5.9	5.7	+	nonRsp	NR
16	F	44	1b	31	2	2	5.5	5.3	4.7	+	nonRsp	NR
17	M	51	1b	38	2	2	6.5	6.2	5.9	+	nonRsp	NR
18	F	55	1b	97	2	2	6.7	6.3	6.1	+	nonRsp	NR
19	M	59	1b	31	3	2	6.7	5.9	5.7	+	nonRsp	NR
20	F	53	1b	71	3	2	5.9	5.8	5.8	+	nonRsp	NR
21	F	51	-	18	0	0	-	-	-	-	-	-
22	F	78	-	13	0	0	-	-	-	-	-	-
23	M	75	-	20	0	0	-	-	-	-	-	-
24	M	34	-	12	0	0	-	-	-	-	-	-
25	M	64	-	30	0	0	-	-	-	-	-	-
26	M	78	-	9	0	0	-	-	-	-	-	-
27	M	53	-	19	0	0	-	-	-	-	-	-
28	F	64	-	12	0	0	-	-	-	-	-	-
29	F	60	-	20	0	0	-	-	-	-	-	-
30	M	66	-	26	0	0	-	-	-	-	-	-

SVR, sustained viral response; NR, nonresponse; Rsp, viral responder, patients with SVR or TR; nonRsp, non-viral responder; patients with NR.

Preparation of liver tissue samples

Liver biopsy samples were taken from all the patients at around 1 week before treatment and at 1 week after starting therapy (Fig. 1A). The biopsy samples were divided into three parts: the first part was immersed in formalin for histological assessment, the second was immediately frozen in liquid nitrogen tank for future RNA isolation, and the final part was frozen in OCT compound for LCM analysis and stored at −80 °C until use. As a control, a liver tissue sample was surgically obtained from a patient who showed no clinical signs of hepatitis and was analyzed as described previously [11].

CLL and CPA were isolated by LCM using a CRI-337 (Cell Robotics, Albuquerque, NM, USA) (Supplementary Fig. 1) from the liver biopsy specimens frozen in OCT compound. The detailed procedure for LCM is described in the Supplementary materials and methods and was performed as previously described [11,19].

RNA isolation and Affymetrix gene chip analysis

Total RNA in each liver biopsy specimen was isolated using the RNAqueous® kit (Ambion, Austin, TX, USA). Total RNA in the specimens frozen for LCM was isolated with a carrier nucleic acid (20 ng poly C) using RNAqueous®-Micro (Ambion). The quality of the isolated RNA was estimated after electrophoresis using an Agilent 2001 Bioanalyzer (Palo Alto, CA, USA). Aliquots of total RNA (50 ng) isolated from the liver biopsy specimens were subjected to amplification with the WT-Ovation™ Pico RNA Amplification System (NuGen, San Carlos, CA, USA) as recommended by the manufacturer. About 10 μg of cDNA was amplified from 50 ng total RNA, and 5 μg of cDNA was used for fragmentation and biotin labeling using the FL-Ovation™ cDNA Biotin Module V2 (NuGen) as recommended by the manufacturer. The biotin-labeled cDNA was suspended in 220 μl of hybridization cocktail (NuGen), and 200 μl was used for the hybridization. Half of the total RNA isolated from the LCM specimens was amplified twice with the TargetAmp™ 2-Round Aminoallyl-aRNA Amplification Kit 1.0 (EPICENTRE, Madison, WI, USA). Twenty-five micrograms of amplified antisense RNA were used for biotin labeling according to the manufacturer's protocol *Biotin-X-X-NHS* (provided by EPICENTRE). The biotin-labeled aRNA was suspended in 300 μl of hybridization cocktail (Affymetrix Inc., Santa Clara, CA, USA), and 200 μl was used for the hybridization with the Affymetrix Human 133 Plus 2.0 microarray chip containing 54,675 probes. After stringent washing, the microarray chips were stained with streptavidin–phycoerythrin, and probe hybridization was determined using a GeneChip® Scanner 3000 (Affymetrix). Data files (CEL) were obtained with the GeneChip® Operating Software 1.4 (GCOS) (Affymetrix). All the expression data were deposited in Gene Expression Omunibus (GEO; http://www.ncbi.nlm.nih.gov/geo/) (NCBI) and the accession ID is GSM 425,995. The experimental procedure is described in detail in the Supplementary materials and methods.

Research Article

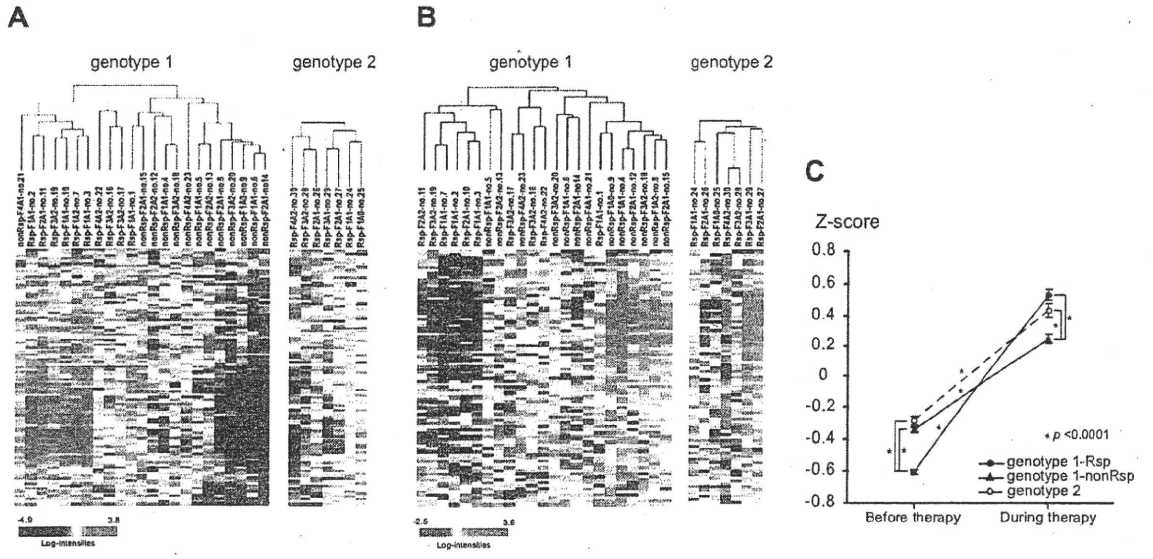

Fig. 1. (A) Hierarchical clustering of expression in genotype 1 and genotype 2 patients during treatment according to fold induction of IRSGs. (B) Hierarchical clustering of expression in genotype 1 and genotype 2 patients before treatment. (C) Serial changes in standardized expression values (Z-score) of IRSGs from genotype 1-Rsp, genotype 1-nonRsp, and genotype 2 patients before and during treatment.

Statistical and pathway analysis of gene chip data

Statistical analysis and hierarchical clustering were performed by BRB-ArrayTools (http://linus.nci.nih.gov/BRB-ArrayTools.htm). A class comparison tool based on univariate or paired *t*-tests was used to find differentially expressed genes (p <0.005). To confirm statistical significance, 2000 random permutations were performed, and all of the *t*-tests were re-computed for each gene. The gene set comparison was analyzed using the BioCarta and the KEGG pathway data bases. The Fisher and Kolmogorov–Smirnov tests were performed for statistical evaluation (p <0.005) (BRB-ArrayTools). Functional ontology enrichment analysis was performed to compare the Gene Ontology (GO) process distribution of differentially expressed genes (p <0.05) using MetaCore™ (GeneGo, St. Joseph, MI, USA).

For the comparison of standardized expression values among different pathway groups, standard units (Z-score) of each gene expression value were calculated as:

$$Z_i = \frac{X_i - X_m}{S}$$

where X_i is the raw expression value, X_m is the mean of the expression values in the pathway, and S is the standard deviation of the expression values.

The standard units in each pathway were expressed as mean ± SEM. A *P*-value of less than 0.05 was considered significant. Multivariate analysis was performed using a logistic regression model with a stepwise method using JMP7 for Windows (SAS Institute, Cary, NC, USA).

Quantitative real-time detection (RTD)-PCR

We performed quantitative real-time detection PCR (RTD)-PCR using TaqMan Universal Master Mix (PE Applied Biosystems, CA). Primer pairs and probes for Mx1, IFI44 and IFITM1, and GAPDH were obtained from TaqMan assay reagents library (Applied Biosystems, CA).

Results

Serial changes in HCV-RNA after initiation of IFN-α 2b and Rib combination therapy

Serial changes in HCV-RNA were monitored at 48 h, 2 weeks, and 24 weeks after the initiation of therapy (Table 1). The biphasic viral decline after the initiation of IFN therapy has been characterized [14,15,18]. We calculated the first phase decline by comparing viral load before therapy and after 48 h, and the second phase decline by comparing viral load after 48 h and 2 weeks (Table 1) [14,15,18]. Both the first and the second phase declines could be associated with treatment outcome and interestingly, viral responders (Rsp) who achieved SVR or TR showed more than a 1-log drop of first phase decline (Log/24 h) and more than a 0.3-log drop of second phase decline (Log/w) (Table 1). In contrast, non-responders (nonRsp) who exhibited NR failed to meet the criteria. The first phase decline of Rsp and nonRsp were 1.38 ± 0.65 log/24 h and 0.77 ± 0.44 log/24 h (p = 0.005), respectively. The second phase decline of Rsp and nonRsp were 0.71 ± 0.34 log/w and 0.11 ± 0.34 log/w (p = 0.0001), respectively. Therefore, the classification of Rsp or nonRsp according to the treatment outcome might be feasible based on the viral kinetic responses to IFN. All but one patient infected with genotype 2 HCV eliminated the virus within 2 weeks. There were no significant differences in the degree of histological activity or staging, nor in the sex, age, or alanine aminotransferase (ALT) level among these patients (Table 1). The amount of HCV-RNA was significantly lower in genotype 2 patients (4.06 ± 0.32 log IU/ml) than in genotype 1 patients (5.70 ± 1.10 log IU/ml) (Table 1).

Identification of IFN-α 2b plus Rib-induced genes in the livers of patients with chronic hepatitis C infection

To identify the genes induced in the liver by combination treatment with IFN-α 2b plus Rib, the gene expression profiles from samples taken around 1 week before and 1 week after initiation of therapy were compared. The pairwise *t*-test comparison showed that 798 genes were up-regulated and 220 genes were down-regulated significantly (p <0.005). The 100 most up-regulated genes according to p values were selected; these are listed in Supplementary Table 1. Many of the interferon-stimulated

genes (ISGs), such as Myxovirus (influenza virus) resistance 1 (MX), 2′,5′-oligoadenylate synthetase (OAS), chemokine (C–C motif) ligand 8 (CCL8), and interferon alpha-inducible protein 27 (IFI 27), were significantly induced (Supplementary Table 1). We designated these genes as *IFN and Rib-stimulated genes* (IRSGs) and analyzed them further.

Hepatic gene expression and responsiveness to IFN-α 2b and Rib combination therapy

To investigate the relationship between hepatic gene expression and responsiveness to treatment, we applied nonsupervised learning methods, hierarchical clustering analysis using all the expressed genes ($n = 34,988$) from samples taken before and 1 week after initiation of therapy. While hierarchical clustering analysis did not form clusters when done for all patients, it formed two clusters – Rsp and nonRsp – when performed within genotype 1 patient (data not shown).

Fold changes in expression in the 100 most up-regulated IRSGs, before and during therapy, were calculated and subjected to hierarchical clustering, and this clearly differentiated Rsp, which exhibited higher IRSGs induction, from nonRsp, as shown in Fig. 1A and Supplementary Table 1. Despite the rapid virus decline in genotype 2 patients, IRSG induction was not so evident in these patients.

Unexpectedly, the hierarchical clustering of IRSG expression in samples taken before treatment showed a reverse pattern of gene expression (Fig. 2B): IRSG induction was significantly higher in nonRsp than in Rsp. Upon treatment, the expression of IRSGs was more induced in Rsp than in nonRsp (Fig. 1C).

The findings were confirmed in patients who were administered Peg-IFN-α 2b and Rib combination therapy (Table 2). IRSG expression was induced in CH-C infected livers and substantially up-regulated in nonRsp compared with Rsp (Supplementary Fig. 1). Multivariate logistic analysis including age, sex, fibrosis stage, activity, HCV-RNA, genotype, treatment regime, ALT and

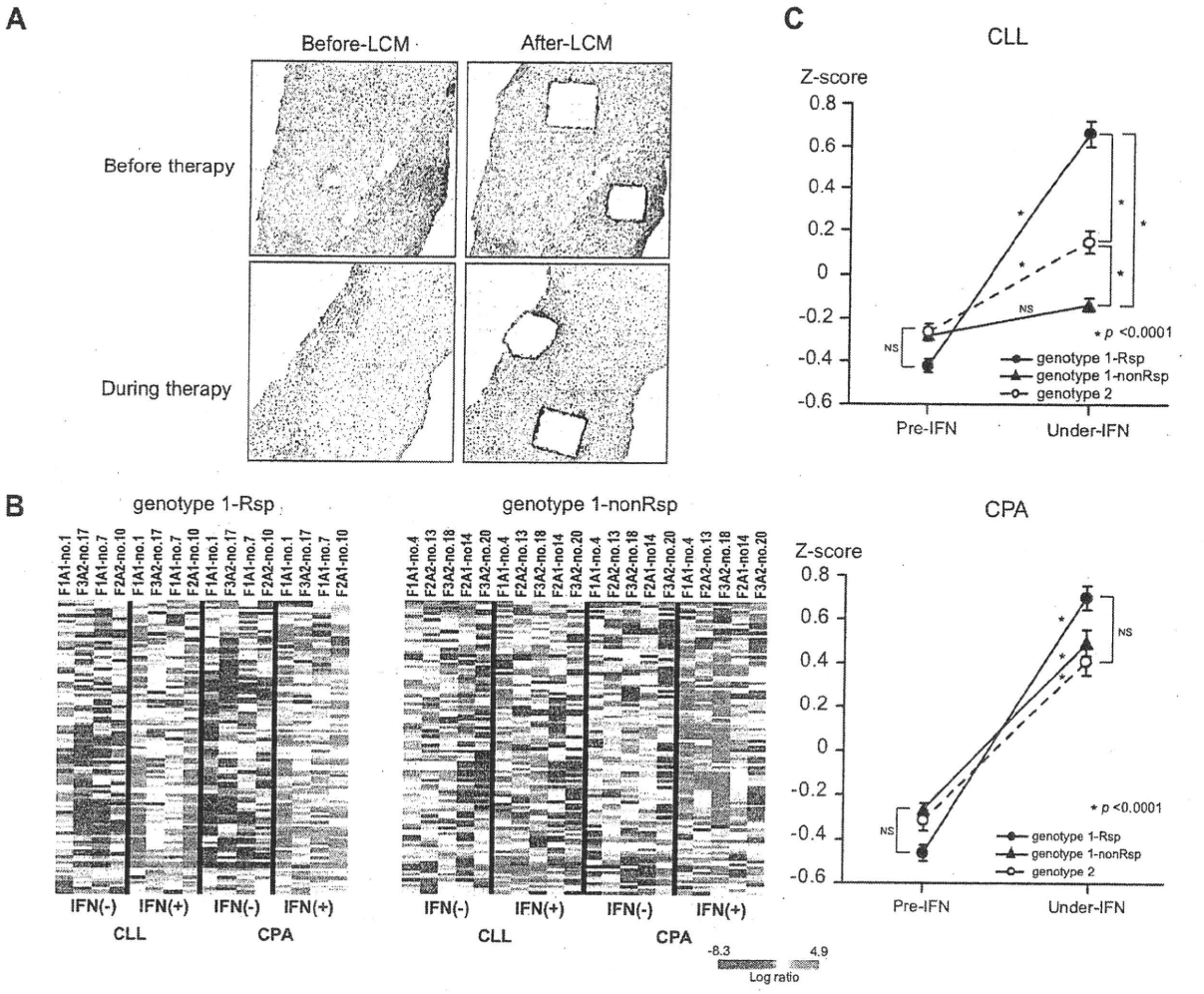

Fig. 2. (A) LCM of liver biopsy samples before and during treatment. (B) Heat map of gene expression of IRSGs in CLL and CPA before and during treatment. (C) Serial changes in standardized expression values (Z-score) of IRSGs in CLL and CPA from genotype 1-Rsp, genotype 1-nonRsp, and genotype 2 patients before and during treatment.

Research Article

expression pattern of IRSGs (up or down) of the 50 patients before treatment showed that genotype 2 ($p < 0.0001$, Odds = 4×10^7) and down-regulated IRSGs ($p < 0.0001$, Odds = 71.2) are significant variables associated with SVR.

Gene expression analysis in cells in liver lobules (CLL) and portal area (CPA)

To explore these findings in more detail, we examined the gene expression profiles of CLL and CPA that had been isolated separately from whole liver biopsy specimens of 12 patients, using the LCM method before and during treatment (Fig. 2A). The representative differentially expressed genes between CLL and CPA are shown in Supplementary Tables 2-1 and 2-2. In CLL, liver-specific proteins and enzymes, such as cytochrome P450, apolipoprotein, and transferrin, were all expressed. In CPA, cytokines, chemokines and lymphocyte surface markers, such as chemokine (C-X-C motif) receptor 4, interleukin-7 receptor and CD83 antigen, were all expressed (Supplementary Tables 2-1 and 2-2). The results confirmed our previous speculation that cells from the lobular area were mostly of hepatocyte origin and that those from the portal area were mostly of liver-infiltrating lymphocyte origin [11,19].

IRSG expression in CLL and CPA from genotype 1-Rsp and non-Rsp is shown in Fig. 2B. In genotype 1-Rsp, IRSG expression was significantly induced in both CLL and CPA by the treatment (Fig. 2B and C). On the other hand, in genotype 1-nonRsp and genotype 2, IRSG induction was impaired especially in CLL, while

Table 3. Up- and down-regulated pathways by gene set comparison between Rsp and nonRsp of genotype 1 patients before therapy (BRB-array tool).

Pathway	No. of genes	LS *p* value	KS *p* value	Representative Genes	Mean probe intensity of representative genes		
					Rsp (n = 20)	nonRsp (n = 23)	Normal (n = 10)
Up-regulated in slow viral drop							
IFN alpha signaling pathway	21	0.00001	0.00300	STAT1	1608	3117	686
				IRF9	1249	1842	614
				IFNAR2	1892	1988	903
Apoptotic Signaling in Response to DNA Damage	55	0.00001	0.07974	CASP3	675	870	426
				CASP7	1165	1510	1264
				CASP9	355	403	264
				TP53	1465	1797	1028
Toll-like receptor signaling pathway	150	0.00006	0.06659	CXCL10	1922	3979	193
				CXCL11	176	321	51
				MYD88	1022	1372	723
				TIRAP	582	722	447
Wnt signal pathway	55	0.00009	0.16058	EIF2AK2	664	1190	484
				CCND1	2439	3558	1162
				APC	143	186	154
				PIK3R1	1570	1906	682
Antigen processing and presentation	139	0.00117	0.00091	TAP2	169	317	93
				HLA-A	11005	14726	6221
				HLA-B	13144	17942	6823
				HLA-C	1937	3993	783
Jak-STAT signaling pathway	220	0.00180	0.13154	STAT2	716	1065	274
				IL28RA	390	544	204
				IL10RB	398	506	338
Down-regulated in slow viral drop							
Metabolism of xenobiotics by cytochrome P450	98	0.00018	0.00082	CYP3A4	15219	10118	19256
				CYP2E1	29129	24549	30929
				AKR1C4	6126	4898	6671
Fatty acid metabolism	88	0.00480	0.05373	ACADL	826	687	785
				ALDH2	18325	16337	21844
				HSD17B4	9619	8807	10653
				ACAD11	6858	6238	8279
				ACOX1	6988	5862	8279

No. of genes, the number of genes comprising the pathway, Rsp, viral responder, patients with SVR or TR; nonRsp, non-viral responder; patients with NR.

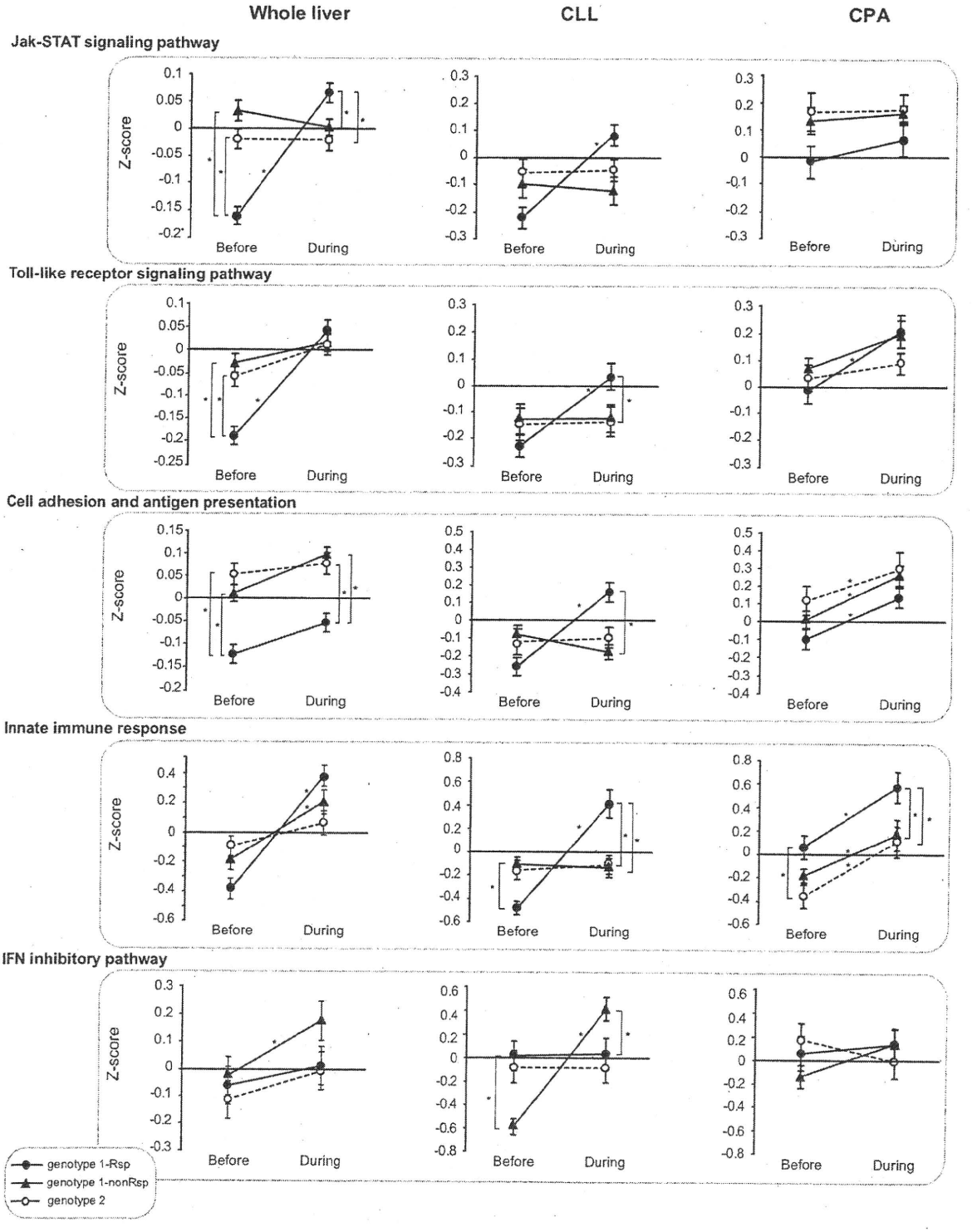

Fig. 3. Serial changes in standardized expression values (Z-score) of differentially expressed pathways from genotype 1-Rsp, genotype 1-nonRsp, and genotype 2 patients before and during treatment in whole liver, CLL, and CPA.

Research Article

it was nearly preserved in CPA from three of five patients (Fig. 2B and C). Thus, IRSG induction in CLL could play an essential role in the eradication of the virus in genotype 1 CH-C patients.

Pathway analysis of gene expression in the livers of genotype 1-Rsp, genotype 1-nonRsp and genotype 2

To explore which signaling pathway contributed to the impaired IRSG induction, pathway comparisons between genotype 1-Rsp ($n = 20$) and genotype 1-nonRsp ($n = 23$) before treatment were performed (Table 3). Gene set comparison was analyzed based on the database of BioCarta and KEGG pathways. The Fisher and Kolmogorov–Smirnov tests were performed for statistical evaluation ($p < 0.005$) (BRB-ArrayTools). The mean probe intensities of representative genes in individual pathways are shown in Table 3. In genotype 1-nonRsp, the signaling pathways of IFN-α, apoptosis, and many of the immune pathways, such as those involved in antigen presentation, and the toll-like receptor (TRL) and Jak-STAT signaling pathways, were generally expressed at significantly higher levels before treatment than genotype 1-Rsp (Table 3 and Fig. 3). During treatment, the immune pathways were significantly up-regulated in genotype 1-Rsp, while they were not up-regulated in genotype 1-nonRsp and genotype 2 (Fig. 3, whole liver). When the CLL and CPA were analyzed separately, significant induction of these pathways was observed in CLL of genotype 1-Rsp but not of genotype 1-nonRsp and genotype 2 (Fig. 3, CLL). However, similar induction patterns were observed in CPA among genotype 1-Rsp, genotype1-nonRsp, and genotype 2 patients (Fig. 3, CPA). Thus, these immune pathways should be activated in CLL for the elimination of virus.

We then evaluated the extent of the innate immune response to treatment. The expression of 10 innate immune response genes was strongly induced in CLL from patients of genotype 1-Rsp but not from genotype 1-nonRsp and genotype 2 patients, although these genes were similarly induced in CPA among these patients (Supplementary Table 3 and Fig. 3).

To examine which signaling pathways were differentially induced during treatment, we utilized MetaCore™. MetaCore™ is more feasible for pathway analysis using a relatively low number of cases, and was therefore selected to analyze the LCM samples in this study. The network processes involving genes for which the differential expression was statistically significant ($p < 0.05$) in genotype 1 patients are shown in Fig. 4. Before treatment, many of the immune mediated pathways, such as IFN-α, cell adhesion, IFN-γ, and TCR, were up-regulated in whole liver specimens from genotype 1-nonRsp compared with Rsp. Similar

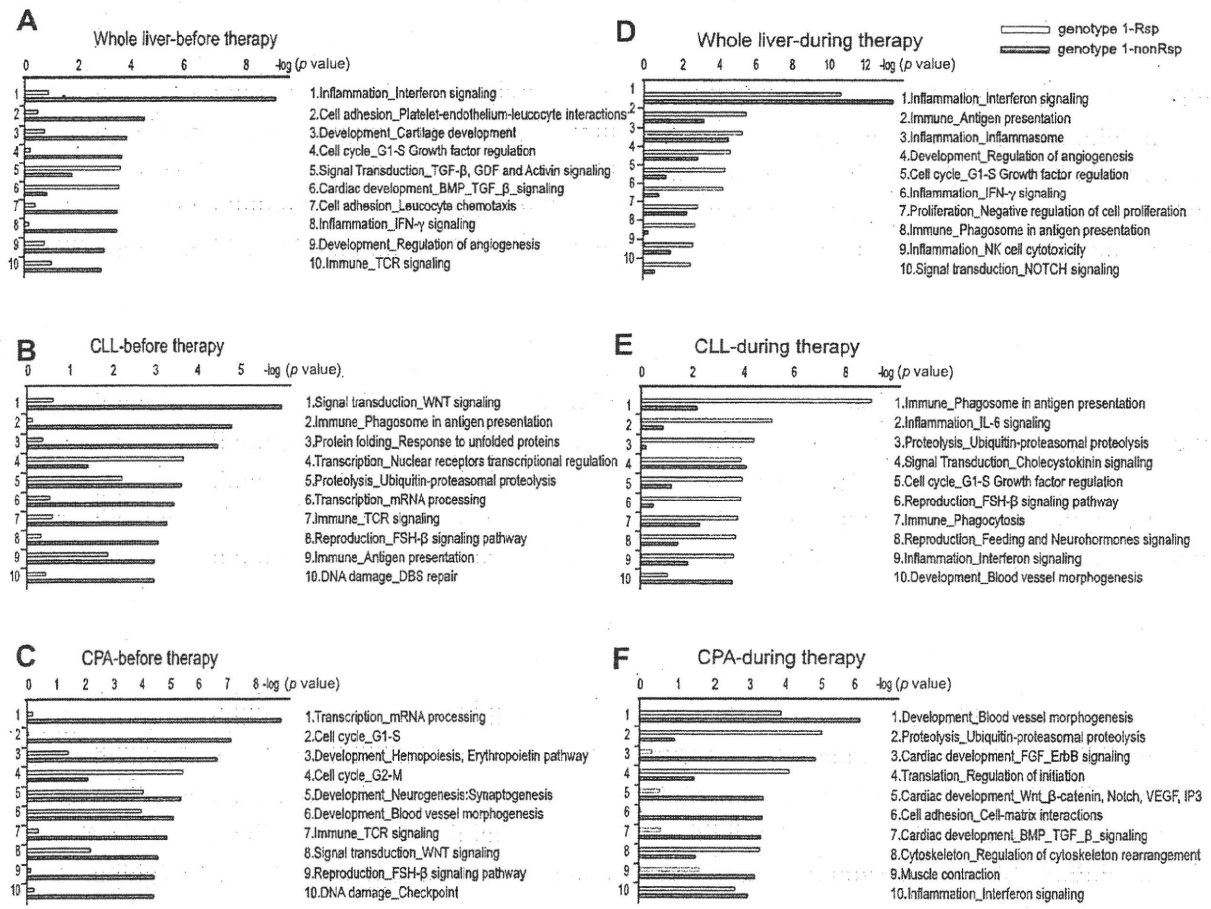

Fig. 4. Functional ontology enrichment analysis of differentially expressed genes ($p < 0.05$) using MetaCore™. GeneGo network process of differentially expressed genes between genotype 1-Rsp (white bar) and genotype 1-nonRsp (blue bar) are listed in order of decreasing statistical significance.

immune-mediated pathways were up-regulated in CLL of genotype 1-nonRsp. In CPA, many of the pathways associated with cell proliferation and DNA damage were up-regulated, reflecting the active inflammatory process in the lymphocytes of genotype 1-nonRsp (Fig. 4A–C). During treatment, many of the immune reactive pathways, such as IFN, NK cell, and antigen presenting, were induced in the whole liver and CLL specimens from genotype 1-Rsp but not in nonRsp (Fig. 4D and E). In contrast, the expression of IFN-inhibitory genes was significantly induced in CLL from nonRsp during treatment (Table 3 and Fig. 4). Interestingly, in CPA, the IFN pathway was induced in genotype 1-Rsp and nonRsp to the same degree; however, signaling pathways related to angiogenesis and fibrogenesis, such as FGF, Wnt, TGF-beta, Nocth, and VEGF signaling, were induced more in CPA from genotype 1-nonRsp than from Rsp (Figs. 3 and 4F). Thus, differential expression of signaling pathways could be observed in CLL and CPA obtained from genotype 1-Rsp and nonRsp.

Discussion

IFN and Rib combination therapy has become a commonly used modality for treating patients with CH-C, although the precise mechanism of treatment resistance is unclear. With the development of methods to quantitatively assess viral kinetics during treatment, studies were able to demonstrate that patients who cleared HCV in the early period showed favorable outcomes, whereas patients who needed a longer time to clear HCV experienced poor outcomes [4,7,17]. Thus, early clearance of virus after initiation of treatment is one of the important determinants for the complete eradication of HCV.

In this study, we analyzed gene expression from liver biopsy samples obtained before and at 1 week after initiation of treatment to investigate the precise mechanisms involved in treatment and treatment resistance. Although global gene expression profiles in the liver and PBMC during IFN treatment in a chimpanzee have been reported [12,13], the relationship between the expression profiles and clinical outcome could not be evaluated.

During the preparation of this study, two reports using a similar approach have been published [6,20]. For example, Feld et al. [6] analyzed gene expression in the livers of CH-C patients on treatment. The authors, however, compared gene expression among different patients at initiation ($n = 19$; 5 rapid responders, 10 slow responders, 4 naive) and during treatment ($n = 11$; 6 rapid responders, 5 slow responders). Because patients were not serially biopsied before and during the treatment, true treatment-related gene induction could not be evaluated. Moreover, half of the on-treatment group was administered Rib alone for three days prior to liver biopsy. In the other report, Sarasin-Filipowicz et al. [20] extensively analyzed serial liver biopsy specimens under the treatment; however, the number of the patients enrolled in their study was relatively low and heterogeneous with respect to the infected genotypes. Our study has extended their findings and provides further insights into the mechanism of IFN resistance by analyzing gene expression in CLL and CPA separately for the first time. The analysis of genotype 2 HCV also enabled us to understand the importance of the differing sensitivities to IFN between strains.

By comparing gene expression in serial liver biopsy specimens obtained at initiation and during treatment, IFN- and Rib-stimulated genes (IRSGs) in the livers of patients with CH-C could be identified (Supplementary Table 1). Our study clearly demonstrated that IRSG induction correlated with the elimination of HCV in patients with genotype 1 in accordance with previous results [6,20]. The patients who did not show a response to treatment had poor induction of IRSGs (Fig. 1A). In contrast, IRSG expression before treatment showed an opposite pattern of expression. IRSGs were induced in genotype 1-nonRsp rather than in genotype 1-Rsp. This finding was first described by Chen et al. [3] and confirmed by others [1,6,20]. Asselah et al. [1] extensively analyzed 58 curated ISGs published previously by RTD-PCR and found that three genes (IFI27, CXCL9 and IFI-6–16) were predictive of treatment outcome. However, only 12 of their 58 curated genes were also included in the 100 most up-regulated genes we observed during treatment (Supplementary Table 1). Therefore, more valuable genes for the prediction of treatment outcome might exist and our gene list could be useful for further selection of predictors of treatment outcome.

We showed that different levels of IRSG induction before treatment was associated with up-regulation of different signaling pathways, such as apoptosis and inflammatory pathways, in genotype 1-nonRsp, although histological assessment of activities and stages could not differentiate the two groups of patients. During treatment, these pathways, including the innate immune response for IFN production, were significantly induced in genotype 1-Rsp but not in genotype 1-nonRsp. The results suggest that previous up-regulation of IRSGs might be linked to impaired induction of IRSGs and contribute to poor treatment response in patients with genotype 1. Interestingly, an impaired IRSG induction was mainly noticeable in CLL, but not in CPA, and the results were confirmed by RTD-PCR (data not shown). These results suggest that IRSG induction in HCV-infected hepatocytes could play an essential role in the eradication of the genotype 1 virus in CH-C patients.

However, these scenarios did not apply in patients with genotype 2 HCV in this study. Despite the presence of active inflammation before treatment and unsatisfactory IRSG induction during treatment, these patients showed rapid responses to treatment and favorable treatment outcomes. It could be speculated that genotype 2 HCV is far more sensitive to IFN than genotype 1 HCV, and small IRSG induction might be enough to eradicate the virus. Further studies are needed to confirm these results.

We precisely analyzed the expression profiles in CLL and CPA which were obtained using the LCM method. Although IRSGs and other immune regulatory genes were similarly induced in the CPA of genotype 1-Rsp and nonRsp, more of the angiogenic- and fibrogenic-related genes were induced in CPA of genotype 1-nonRsp (Fig. 4C and F). Therefore, growth factors released from CPA might be involved in poor IRSG induction in CLL of genotype 1-nonRsp.

In summary, by comparing the hepatic gene expression in CH-C patients with different treatment outcomes, we identified a gene expression signature characteristic of IFN resistance. Our study is very important for two reasons: first, it will help in the development of new therapeutic strategies, and second, we have identified many of the genes found to be up-regulated between genotype 1-Rsp and nonRsp, which encode molecules secreted

Research Article

in serum (cytokines). Therefore, the study represents a logical functional approach for the development of serum markers as predictors of response to treatment [2]. The precise mechanisms underlying these findings should be clarified further in future studies.

Conflict of interest

The authors who have taken part in this study do not have a relationship with the manufactureres of the drugs involved either in the past or present and did not recieve fundig from the manufactureres to carry out their research. The authors received support from the Japanese Society of Gastroenterology and Ministry of Helath, Labour and Welfare.

Supplementary data

Supplementary data associated with this article can be found, in the online version, at doi:10.1016/j.jhep.2010.04.036.

References

[1] Asselah T, Bieche I, Narguet S, Sabbagh A, Laurendeau I, Ripault MP, et al. Liver gene expression signature to predict response to pegylated interferon plus ribavirin combination therapy in patients with chronic hepatitis C. Gut 2008;57:516–524.
[2] Asselah T, Bieche I, Sabbagh A, Bedossa P, Moreau R, Valla D, et al. Gene expression and hepatitis C virus infection. Gut 2009;58:846–858.
[3] Chen L, Borozan I, Feld J, Sun J, Tannis LL, Coltescu C, et al. Hepatic gene expression discriminates responders and nonresponders in treatment of chronic hepatitis C viral infection. Gastroenterology 2005;128:1437–1444.
[4] Davis GL, Wong JB, McHutchison JG, Manns MP, Harvey J, Albrecht J. Early virologic response to treatment with peginterferon alfa-2b plus ribavirin in patients with chronic hepatitis C. Hepatology 2003;38:645–652.
[5] Desmet VJ, Gerber M, Hoofnagle JH, Manns M, Scheuer PJ. Classification of chronic hepatitis: diagnosis, grading and staging. Hepatology 1994;19: 1513–1520.
[6] Feld JJ, Nanda S, Huang Y, Chen W, Cam M, Pusek SN, et al. Hepatic gene expression during treatment with peginterferon and ribavirin: identifying molecular pathways for treatment response. Hepatology 2007;46: 1548–1563.
[7] Ferenci P, Fried MW, Shiffman ML, Smith CI, Marinos G, Goncales Jr FL, et al. Predicting sustained virological responses in chronic hepatitis C patients treated with peginterferon alfa-2a (40 KDa)/ribavirin. J Hepatol 2005;43: 425–433.
[8] Fried MW, Shiffman ML, Reddy KR, Smith C, Marinos G, Goncales Jr FL, et al. Peginterferon alfa-2a plus ribavirin for chronic hepatitis C virus infection. N Engl J Med 2002;347:975–982.
[9] Germer JJ, Harmsen WS, Mandrekar JN, Mitchell PS, Yao JD. Evaluation of the COBAS TaqMan HCV test with automated sample processing using the MagNA pure LC instrument. J Clin Microbiol 2005;43:293–298.
[10] He XS, Ji X, Hale MB, Cheung R, Ahmed A, Guo Y, et al. Global transcriptional response to interferon is a determinant of HCV treatment outcome and is modified by race. Hepatology 2006;44:352–359.
[11] Honda M, Yamashita T, Ueda T, Takatori H, Nishino R, Kaneko S. Different signaling pathways in the livers of patients with chronic hepatitis B or chronic hepatitis C. Hepatology 2006;44:1122–1138.
[12] Huang Y, Feld JJ, Sapp RK, Nanda S, Lin JH, Blatt LM, et al. Defective hepatic response to interferon and activation of suppressor of cytokine signaling 3 in chronic hepatitis C. Gastroenterology 2007;132:733–744.
[13] Lanford RE, Guerra B, Bigger CB, Lee H, Chavez D, Brasky KM. Lack of response to exogenous interferon-alpha in the liver of chimpanzees chronically infected with hepatitis C virus. Hepatology 2007;46: 999–1008.
[14] Layden TJ, Layden JE, Reddy KR, Levy-Drummer RS, Poulakos J, Neumann AU. Induction therapy with consensus interferon (CIFN) does not improve sustained virologic response in chronic hepatitis C. J Viral Hepat 2002;9:334–339.
[15] Neumann AU, Lam NP, Dahari H, Gretch DR, Wiley TE, Layden TJ, et al. Hepatitis C viral dynamics in vivo and the antiviral efficacy of interferon-alpha therapy. Science 1998;282 (5386):103–107.
[16] Okamoto H, Tokita H, Sakamoto M, Horikita M, Kojima M, Iizuka H, et al. Characterization of the genomic sequence of type V (or 3a) hepatitis C virus isolates and PCR primers for specific detection. J Gen Virol 1993;74: 2385–2390.
[17] Payan C, Pivert A, Morand P, Fafi-Kremer S, Carrat F, Pol S, et al. Rapid and early virological response to chronic hepatitis C treatment with IFN alpha2b or PEG-IFN alpha2b plus ribavirin in HIV/HCV co-infected patients. Gut 2007;56:1111–1116.
[18] Rosen HR, Ribeiro RR, Weinberger L, Wolf S, Chung M, Gretch DR, et al. Early hepatitis C viral kinetics correlate with long-term outcome in patients receiving high dose induction followed by combination interferon and ribavirin therapy. J Hepatol 2002;37:124–130.
[19] Sakai Y, Honda M, Fujinaga H, Tatsumi I, Mizukoshi E, Nakamoto Y, et al. Common transcriptional signature of tumor-infiltrating mononuclear inflammatory cells and peripheral blood mononuclear cells in hepatocellular carcinoma patients. Cancer Res 2008;68:10267–10279.
[20] Sarasin-Filipowicz M, Oakeley EJ, Duong FH, Christen V, Terracciano L, Filipowicz W, et al. Interferon signaling and treatment outcome in chronic hepatitis C. Proc Natl Acad Sci USA 2008;105:7034–7039.
[21] Younossi ZM, Baranova A, Afendy A, Collantes R, Stepanova M, Manyam G, et al. Early gene expression profiles of patients with chronic hepatitis C treated with pegylated interferon-alfa and ribavirin. Hepatology 2009;49:763–774.

MAJOR ARTICLE

La Protein Required for Internal Ribosome Entry Site–Directed Translation Is a Potential Therapeutic Target for Hepatitis C Virus Replication

Takayoshi Shirasaki,[1,2] Masao Honda,[1,2] Hideki Mizuno,[1] Tetsuro Shimakami,[1] Hikari Okada,[1] Yoshio Sakai,[1] Seishi Murakami,[3] Takaji Wakita,[4] and Shuichi Kaneko[1]

[1]Department of Gastroenterology, [2]Department of Advanced Medical Technology, Division of Health Medicine, Graduate School of Medicine, [3]Division of Molecular Cell Signaling, Cancer Research Institute, Kanazawa University, Kanazawa, and [4]Department of Virology II, National Institute of Infectious Diseases, Tokyo, Japan

Background. Translation of the hepatitis C virus (HCV) is mediated by an internal ribosome entry site (IRES). Here, we analyzed the functional relevance of La protein for replication of HCV using an infectious HCV clone, JFH-1.

Methods. A single-nucleotide mutation from A to U was introduced at the 338th nucleotide in the stem-loop domain IV structure of HCV IRES, which stabilized stem-loop IV and abolished translation and replication of JFH-1 almost completely.

Results. During JFH-1 replication, translation initiation factors required for HCV IRES activity, including La protein, polypyrimidine tract binding protein (PTB), PSMA7, and PCBP2, were significantly induced in Huh-7.5 cells. Interestingly, JFH-1 infection increased telomerase activity and induced the expression of human telomerase RNA (hTR) in Huh-7.5 cells. In 37 tissue specimens from patients with chronic hepatitis C, La protein significantly correlated with the representative essential telomerase components hTR, p23, and HSP90 ($P < .001$). Recombinant adenovirus that expressed short-hairpin RNA against La protein successfully suppressed the levels of La protein and core protein of JFH-1 to 30% of that in the control cells.

Conclusions. HCV infection might be strongly related to telomerase activity in the liver through La protein induction. Inhibition of La protein substantially repressed JFH-1 replication; therefore, La protein is a potential therapeutic target for HCV.

Hepatitis C virus (HCV) is a positive-strand, enveloped RNA virus that belongs to the genus *Hepacivirus* in the family *Flaviviridae*. A human liver infected with HCV develops chronic hepatitis, cirrhosis, and in some instances, hepatocellular carcinoma [1]. Although a combination of ribavirin and interferon has become a routine means of treating infected patients, the results are often unsatisfactory, especially in patients with a high viral load [2]. Identification of host factors that regulate HCV replication in infected patients could be helpful in the development of a novel antiviral treatment strategy. It has been reported that various host factors are associated with HCV infection; however, only a few proteins have been functionally shown with an infectious HCV clone to regulate HCV replication [3].

The translation of HCV is initiated by a highly structured RNA segment, the internal ribosome entry site (IRES), which occupies most of the 5′ nontranslated RNA [4]. Many canonical and noncanonical translation initiation factors, such as La protein [5], polypyrimidine tract binding protein (PTB) [6], and eukaryotic initiation factor 3 (eIF3), interact with HCV IRES and might regulate HCV translation. Previously, we reported that HCV IRES activity is highly dependent on these initiation factors, and it correlated with the expression of La protein [7, 8]. However, the functional relevance of these translation initiation factors on HCV

Received 17 September 2009; accepted 6 January 2010; electronically published 24 May 2010.

Potential conflicts of interest: none reported.

Financial support: This study is partially supported by the Grants-in-Aid for Scientific Research by Japan Society for the Promotion of Science (project 17591036).

Reprints or correspondence: Dr Masao Honda, Department of Gastroenterology, Graduate School of Medicine, Kanazawa University, Takara-Machi 13-1, Kanazawa 920-8641, Japan (mhonda@m-kanazawa.jp).

The Journal of Infectious Diseases 2010;202(1):75–85

0022-1899/2010/20201-0009$15.00
DOI: 10.1086/653081

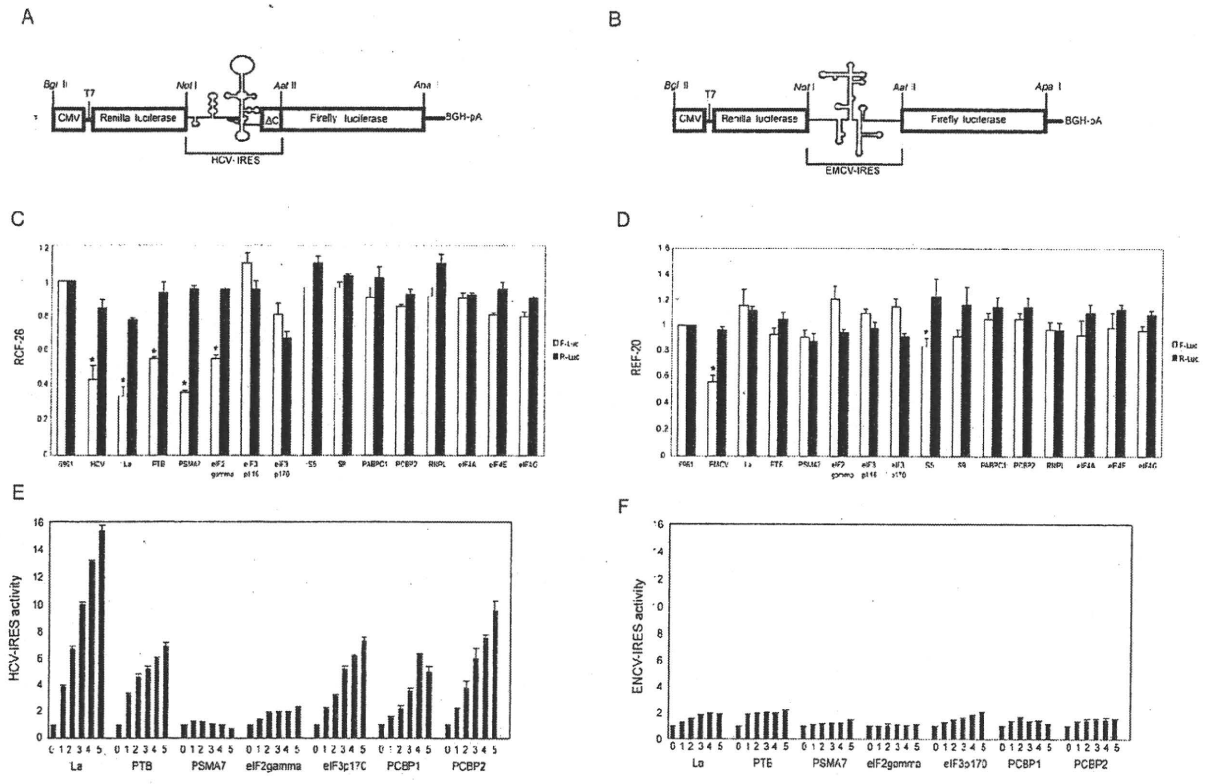

Figure 1. Organization of the transcriptional unit of plasmids pRL-HL (*A*) and pRL-EL (*B*). *C* and *D*, Suppression of 14 canonical and noncanonical initiation factors by specific antisense oligonucleotides. Changes in *Renilla* luciferase (RL) and firefly luciferase (FL) (hepatitis C virus–internal ribosome entry site [HCV-IRES]–directed translation) activities in RCF-26 (*C*). Changes in RL and FL (encephalomyocarditis virus [ENCV]–IRES–directed translation) activities in REF-20 (*D*). $^*P < .05$. *E* and *F*, In vitro translation of pRL-HL and pRL-EL in rabbit reticulocyte lysate. The plasmids pRL-HL or pRL-EL (0.05 μg) and increasing amounts of expression vectors (0–0.125 μg) of La protein, polypyrimidine tract binding protein (PTB), eIF3p 170, eIF2γ, PSMA7, PCBP1, and PCBP2 were co-translated in rabbit reticulocyte lysate. The fold increases in relative HCV IRES activity (*E*) and ENCV-IRES activity (*F*) are shown. $^*P < .05$. *Lane 0*, 0 μg; *lane 1*, 0.025 μg; *lane 2*, 0.05 μg; *lane 3*, 0.075 μg; *lane 4*, 0.1 μg; *lane 5*, 0.125 μg. $^*P < .05$.

replication had not been fully evaluated. In this study, we found that the expression of La protein is induced by HCV infection, and this induced La protein–activated telomerase activity in a human hepatoma cell line. The results indicate La protein is a potential therapeutic target for HCV infection.

EXPERIMENTAL PROCEDURES

Expression vector plasmids. The FLAG tag fusion La protein expression vector (pCMV-La-FLAG) was created by polymerase chain reaction (PCR), using the La protein expression vector (pCMV-La) as the template [8]. The forward primer 5′-AAT GAA ATC AGA AGA AA-3′ contains an *Xba* I site, and the reverse primer 5′-TGA TCT AGA TTA CTT ATC GTC GTC ATC CTT GTA ATC CTG GTC TCC AGC ACC ATT TTC TGT TTT CTG TTG -3′ contains *Xba* I and FLAG sites.

Cell lines. Human hepatocellular carcinoma 7 (Huh-7) cells and Huh-7.5 cells (provided by Professor C. M. Rice, Rockefeller University) were maintained in Dulbecco modified Eagle medium (DMEM; Gibco BRL), which contained 10% fetal bovine serum and 1% penicillin/streptomycin. The RCF-26 was a stably transformed cell line from Huh-7 cells that constitutively expressed dicistronic RNA transcripts containing sequences encoding 2 reporter proteins—*Renilla* luciferase and firefly luciferase—separated by a functional HCV IRES of genotype 1b (Figure 1*A*) [7]. The REF-20 was a stably transformed cell line from Huh-7 cells that constitutively expressed dicistronic RNA transcripts in which HCV IRES was replaced with encephalomyocarditis virus (EMCV) IRES (Figure 1*B*).

Antisense oligodeoxynucleotide. The antisense phosphorothioate oligodeoxynucleotides (oligos) designed for HCV IRES, La protein, PTB, eIF3, eIF2γ, S9, poly(A)-binding protein cytoplasmic 1 (PABPC1), PCBP2, RNPL, and control randomized oligo 6961 were described elsewhere [8]. Antisense oligos for PSMA7, S5, eIF4A, eIF4E, eIF4G, and EMCV IRES were synthesized. The nucleotide sequences of the antisense oligos were 5′-CTC ATG CCG GCG GGC GGC CG-3′ for PSMA7,

5′-GTC ATC CTG AGA ACA CAG CC-3′ for S5, 5′-GAC ATG ATC CTT AGA AAC TA-3′ for eIF4A, 5′-GCC ATC TTA GAT CGA TCT GA-3′ for eIF4E, 5′- GAC ATG ATC TCC TCT GTG AT-3′ for eIF4G, and 5′-TCC ATA TTA TCA TCG TGT TT-3′ for EMCV IRES. The antisense oligos (1.0 μmol/L) were transfected into RCF-26 (Figure 1*C*) or REF-20 (Figure 1*D*). After 24 h of transfection, *Renilla* luciferase (cap-dependent translation) and firefly luciferase (HCV or EMCV-directed translation) activities were measured with the Dual-Luciferase Reporter Assay System (Promega).

In vitro translation of pRL-HL and pRL-EL in rabbit reticulocyte lysate. In vitro translation of pRL-HL and pRL-EL was carried out in transcription and translation–coupled rabbit reticulocyte lysate systems (Promega). In 25 μL of the transcription and translation reaction mixture, 0.05 μg of pRL-HL or pRL-EL was cotranslated with an increasing amount of plasmid DNA (up to 0.125 μg) of La, PTB, PSMA7, eIF2-γ, eIF3p170, PCBP1, and PCBP2, which were cloned using the T7 promoter. A 3-μL aliquot was then used to measure *Renilla* luciferase and firefly luciferase activities using the Dual-Luciferase Reporter Assay System (Promega).

Site-directed mutagenesis. The plasmid pJFH-1 was used as the template for introduction of the site-directed mutation at nucleotide 338 in the 5′ nontranslated RNA. The site-directed mutagenesis reaction was performed using the Pfu Turbo DNA polymerase PCR system (Stratagene), according to the manufacturer's instructions.

Transfection of JFH-1 and JFH-1 338U into Huh-7.5 cells. Ten micrograms of synthetic RNA transcribed from pJFH-1 or pJFH-1 338U was used for electroporation. Cells were then pulsed at 260 V and 950 μF using the Gene Pulser II apparatus (Bio-Rad Laboratories).

Infection of Huh-7.5 cells with JFH-1. Seventy-two hours after transfection, the culture medium was collected, cleared by low-speed centrifugation at 2000 revolutions per minute at 760*g* for 10 min, and passed through a Millipore filter (pore size, 0.45 μm; Millipore Corporation). Part of the filtered culture medium was diluted 50-fold or 10-fold with DMEM containing 10% fetal bovine serum and 1% penicillin-streptomycin. Diluted culture medium (1 mL) was used for injection of cells into a well of a 6-well plate or a well containing cover slips and incubated for 4 h. At 3 days after infection, inoculated cells grown on cover slips were fixed and stained using anti-core antibody, as described below. The amounts of HCV RNA, La-RNA, and human telomerase RNA (hTR)-RNA in inoculated cells were determined by quantitative real-time detection (RTD)-PCR.

Western blot analysis and immunofluorescence staining. The expression levels of La protein and PTB in cells were evaluated by Western blotting using mouse anti-La antibody (SW5) and rabbit anti-PTB antibody, as described elsewhere [9]. The expression of HCV core protein, PSMA7, eIF2γ, PCBP2, and FLAG-tagged La protein was evaluated with mouse anti-core antibody (Affinity BioReagents), mouse anti-PSMA7 antibody (Antibodies Direct), rabbit anti-eIF2γ antibody (Abcam), mouse anti-huRNP E2 (23-G) antibody (Santa Cruz Biotechnology), and mouse anti-FLAG antibody (Sigma), respectively. For immunofluorescence staining, anti–core monoclonal antibodies and Alexa Fluor 488 goat anti–mouse immunoglobulin G antibody (Invitrogen) were used.

Quantitative RTD-PCR. The primer pairs and probes for La protein, PTB, eIF3 p170, GAPDH, and HCV were obtained as described elsewhere [8]. The primer pairs and probes for PSMA7, eIF2γ, PCBP2, hTR, p23, Hps90, and β-actin were obtained from the TaqMan assay reagents library. One microgram of isolated RNA was reverse-transcribed to complementary DNA using SuperScript II RT (Invitrogen) according to the manufacturer's instructions, and the resulting complementary DNA was amplified with appropriate TaqMan assay reagents [10].

Telomerase activity assay. The plasmids pCMV-La-FLAG and pCR3.1 were transfected into Huh-7 cells using Fugene 6 transfection reagent (Roche Applied Science). Forty-eight hours after transfection, the amounts of hTR-RNA in the transfected cells were determined by RTD-PCR. The expression of the FLAG-tag fusion La protein was evaluated by Western blot analysis. Telomerase activity was measured with a PCR-based telomerase repeat amplification protocol (TRAP) assay, performed with the TRAPEZE kit (Invitrogen) according to the manufacturer's instructions. Each reaction product was amplified in the presence of a 36-base pair internal telomerase assay standard. The PCR products were fractionated by electrophoresis on a 10% polyacrylamide gel and then visualized by staining with SYBR Green (Molecular Probes).

Construction of recombinant adenovirus expressing short-hairpin RNA for La protein. The short-hairpin RNA expression plasmid (pSh-La), which expresses short-hairpin RNA for La protein (seq: 5′-CCG GCC AAG GCA GAA CTC ATG GAA ACT CGA GTT TCC ATG AGT TCT GCC TTG GTT TG-3′), was purchased from Sigma. The pSh-La was digested with the enzymes *Hind* III and *Bam*HI, and the excised fragment, including the short-hairpin RNA, was transferred to the adenoviral expression plasmid. The adenoviral expression plasmid and bovine growth hormone plasmid were cotransfected into 293A cells using the CellPhect Transfection kit (GE Healthcare) to produce crude adenoviral stocks. These stocks were purified using the Adeno-X Virus Purification kit (Clontech Laboratories) and stored at −80°C. The titers of the adenoviral stocks were adjusted to 4.0×10^9 PFU/mL.

Twelve hours after JFH-1 RNA transfection, the cells were washed 3 times with phosphate-buffered saline, and then Ad-shLa or Ad-Null was added at a multiplicity of infection of 10.

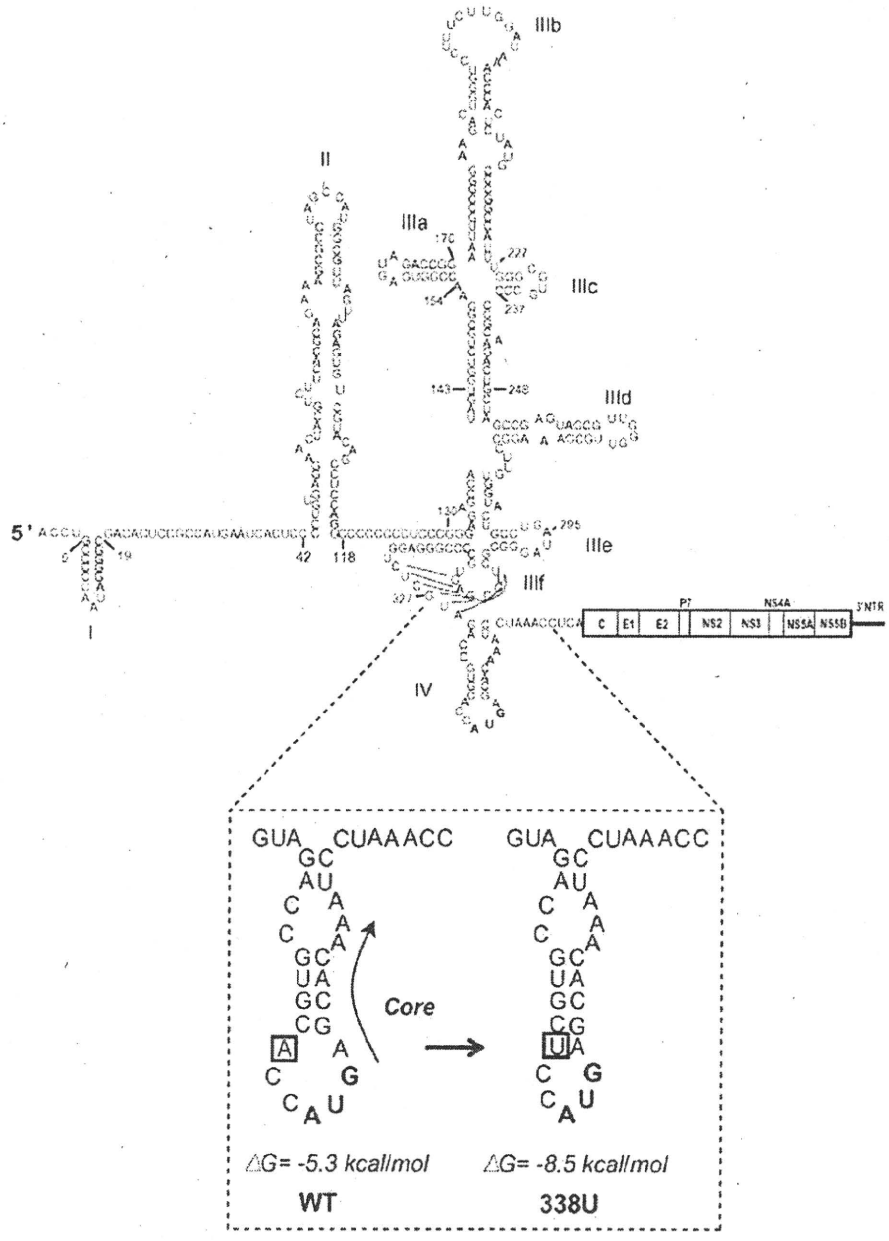

Figure 2. Organization of the full-length JFH-1 and the mutation at nucleotide 338 of stem loop IV.

One hour after injection, the cells were washed 3 times with phosphate-buffered saline, and complete culture medium was added.

Statistical analysis. Results were expressed as mean values ± standard deviation. Significance was tested by 1-way analysis of variance with Bonferroni methods, and differences were considered statistically significant at $P < .05$.

RESULTS

Dependence of HCV IRES activity on translation initiation factors. To confirm that HCV IRES activity was highly dependent on translation initiation factors, antisense oligonucleotides designed for 14 translation initiation factors were transfected into RCF-26 and REF-20 cells, and HCV or EMCV IRES

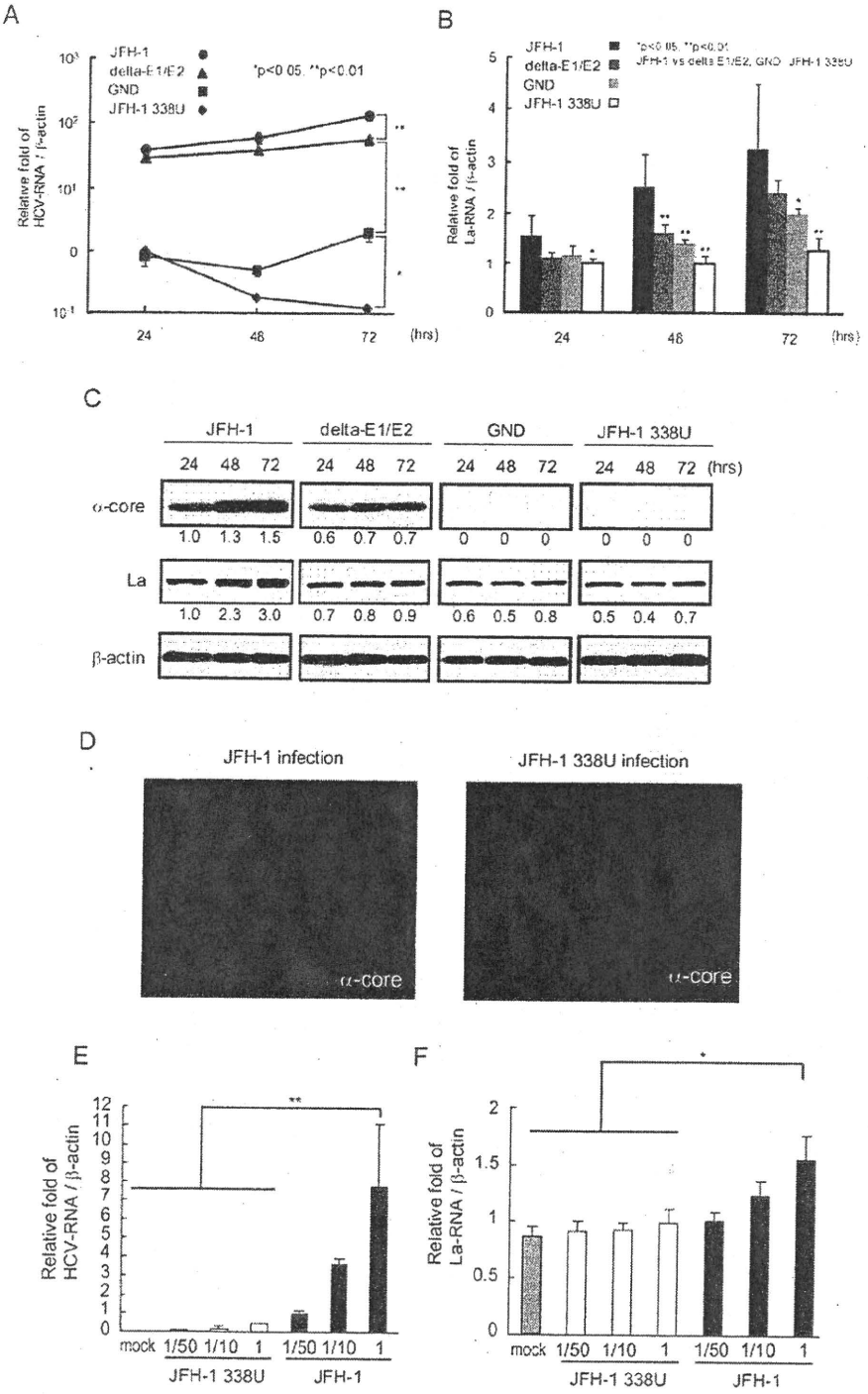

Figure 3. *A*, Hepatitis C virus (HCV) RNA replication determined by real-time detection–polymerase chain reaction (RTD-PCR) in JFH-1, JFH-1/delta E1-E2, JFH-1/GND, and JFH-1 338U transfected cells. $*P < .05$. $**P < .01$. *B*, La RNA expression determined by RTD-PCR in JFH-1, JFH-1/delta E1-E2, JFH-1/GND, and JFH-1 338U transfected cells. $*P < .05$. $**P < .01$. *C*, Western blots for detection of HCV core protein and La protein in JFH-1, JFH-1/delta E1-E2, JFH-1/GND and JFH-1 338U transfected cells. *D*, Immunofluorescence staining of core protein in Huh-7.5 cells infected with JFH-1 or JFH-1 338U. *E* and *F*, HCV RNA and La RNA determined by RTD-PCR in Huh-7.5 cells infected with serial dilution of JFH-1 or JFH-1 338U. $*P < .05$, $**P < .01$.